Impacts of biological parameterization, initial conditions, and environmental forcing on parameter sensitivity and uncertainty in a marine ecosystem model for the Bering Sea

G.A. Gibson [a,*], Y.H. Spitz [b]

[a] International Arctic Research Center, University of Alaska, Fairbanks, AK 99775-7340, USA
[b] College of Oceanic and Atmospheric Sciences, Oregon State University, Corvallis, OR 97331-5503, USA

ARTICLE INFO

ABSTRACT

We use a series of Monte Carlo experiments to explore simultaneously the sensitivity of the *BEST* marine ecosystem model to environmental forcing, initial conditions, and biological parameterizations. Twenty model output variables were examined for sensitivity. The true sensitivity of biological and environmental parameters becomes apparent only when each parameter is allowed to vary within its realistic range. Many biological parameters were important only to their corresponding variable, but several biological parameters, e.g., microzooplankton grazing and small phytoplankton doubling rate, were consistently very important to several output variables. Assuming realistic biological and environmental variability, the standard deviation about simulated mean mesozooplankton biomass ranged from 1 to 14 mg C m^{-3} during the year. Annual primary productivity was not strongly correlated with temperature but was positively correlated with initial nitrate and light. Secondary productivity was positively correlated with primary productivity and negatively correlated with spring bloom timing. Mesozooplankton productivity was not correlated with water temperature, but a shift towards a system in which smaller zooplankton undertake a greater proportion of the secondary production as the water temperature increases appears likely. This approach to incorporating environmental variability within a sensitivity analysis could be extended to any ecosystem model to gain confidence in climate-driven ecosystem predictions.

© 2011 Elsevier B.V. All rights reserved.

1. Introduction

In an era of unprecedented climate change, understanding and predicting the effects of climate variability on marine food webs and marine productivity are of great importance. This is especially true with respect to potential consequences of climate change on commercially important fisheries. The use of hydrographic models coupled to Nutrient–Phytoplankton–Zooplankton–Detritus (*NPZD*) models to describe and predict future marine ecosystem dynamics is an approach that is becoming increasingly widespread. However, biological elements have inherent variability associated with their behavior and, as such, there is some degree of uncertainty surrounding each of the biological model parameters used to describe ecosystem behavior. Any degree of confidence in marine ecosystem projections requires some measure of model sensitivity and uncertainty. Sensitivity analysis can additionally help determine which model parameters are most important in controlling model output. This can help focus efforts during model

tuning to hindcast ecosystem behavior, improve predictive models, and indicate where further efforts from field and laboratory studies would be most beneficial. In-depth sensitivity analysis should be considered a prerequisite for any marine ecosystem model prior to coupling with three-dimensional hydrographic models and higher trophic level models, which will undoubtedly have their own uncertainties.

It has become common practice to use a Monte Carlo type approach (Sobol, 1994) to assess the sensitivity of ecosystem models. Such an approach usually involves an initial first guess for parameter values along with upper and lower limits to specify the parameters' possible domains. Parameter inputs are then randomly selected from their specified domains and used to run the model. Repeating this procedure multiple times allows the model variance and statistical relationship between model parameters and model outputs to be determined. Megrey and Hinckley (2001) used a Monte Carlo approach to assess the influence of turbulence on feeding of larval fishes. In their analysis, biological model parameters were ranked in order of importance using Pearson's R correlations, the premise being the greater the correlation between a parameter and the output variable the more influence the parameter has in controlling model behavior (Rose et al., 1991). Yoshie et al. (2006) used a Monte Carlo approach to perform a sensitivity analysis on the Nemuro *NPZD* model, but they ranked parameters in

* Corresponding author at: International Arctic Research Center, University of Alaska Fairbanks, PO Box 757340, Fairbanks, Alaska, 99775-7340, USA. Tel.: +1 907 474 2768; fax: +1 907 474 5662.
E-mail address: ggibson@iarc.uaf.edu (G.A. Gibson).

order of importance as determined by a normalized sensitivity measure that was based on the fractional change in an output variable relative to the fractional change in a given parameter. Verbeeck et al. (2006), who used a Monte Carlo analysis to determine the sensitivity of a forest carbon flux model, ranked parameters using a Least Squares Linearization (LSL), a multiple regression between the parameters' deviation from the mean and the model output. The advantage of an LSL approach is that it splits output uncertainty into its sources, so the relative contribution of all the parameters to the overall output uncertainty can be assessed.

The behavior of an NPZD model should ideally be explored for parameter sets that encompass the true variability of each of the model parameters. However, the range of possible values for each of the biological model parameters in an NPZD model varies quite considerably with some parameters being well constrained while others are poorly known. Field studies help constrain many of the ecosystem model parameters within a biologically realistic range, but relating measured field values to model parameters is not always straightforward. For example, parameter rates in the model usually represent maxima that are then 'limited' by various factors. By comparison, the observed field values generally reflect the post-limited rates. Laboratory studies, such as rate response to temperature or prey fields, are also useful for constraining parameters and defining functional responses. However, these experiments do not necessarily cover the range of temperatures found in the study region, and the experimental conditions are often gross simplifications of reality (for instance, single species cultures and constant light). Additionally, ecosystem models typically have a few parameters that can only be represented by an educated 'best guess', e.g., 'undefined predation', which is usually treated as a model closure term. This immeasurable parameter is usually parameterized to provide optimum model performance. Due to both known and unknown uncertainties, some model parameters can have a relatively large ($>\pm100\%$ of the mean value) potential range. This presents a challenge when selecting values for use in modeling efforts.

The relative influence of biological and physical forcing to ecosystem model dynamics is of great interest. A full assessment of marine ecosystem sensitivities would require an in-depth sensitivity analysis of coupled three-dimensional physical–biological models in which both biological and physical parameters are varied simultaneously. At present, such analyses are generally limited by computational constraints. However, the inclusion of parameters representative of the physical environment in a sensitivity analysis of a one-dimensional NPZ model could potentially provide numerous insights into the relative importance of biological and physical parameters. Inclusion of such parameters can also provide insights into the likely ecosystem response under alternative physical conditions or in regions different from the one for which the ecosystem model was initially developed.

Here we use a Monte Carlo style analysis to explore the sensitivity of an NPZD type lower trophic level model developed under the Bering Ecosystem Study (BEST) program. This model has been designed for coupling to the Forage-Euphausiid Abundance in Space and Time (FEAST) higher trophic level model under development through the Bering Sea Integrated Ecosystem Research Project (BSIERP, http://bsierp.nprb.org). Using an incomplete factorial design, we explore the relative sensitivity of model dynamics to uncertainty in biological model parameters, initial conditions, and environmental forcing. The approach used in our analysis can be extended to any ecosystem model, and it would provide a measure of confidence to any prediction of ecosystem response.

2. Methods

2.1. Model description

The South East Bering Sea plankton community can be characterized by large and small phytoplankton (Olson and Strom, 2002; Sukhanova, et al., 1999), microzooplankton (Olson and Strom, 2002), large and

small copepods (Coyle et al., 2007; Vidal and Smith, 1986), and euphausiids (Coyle and Pinchuk, 2002). An NPZD model developed for the Gulf of Alaska (Hinckley et al., 2009) with a subarctic ecosystem structure comprising multiple nutrient, phytoplankton, and zooplankton components therefore provided a convenient starting point for the development of the BEST–NPZD model. To adapt the model to the Eastern Bering Sea ecosystem, the model was coupled at the ocean surface to an ice biology module and at the ocean floor to a benthic biology module. A pelagic jellyfish component was also added, and some of the formulations were modified to better describe the Bering Sea ecosystem dynamics. The pertinent changes are outlined in the text below. A schematic of the BEST–NPZD model is shown in Fig. 1. The full set of equations is given in Table 1, with sub-equations in Table 2.

2.1.1. Water column components

2.1.1.1. Nutrients and phytoplankton. The BEST–NPZD follows the temporal change of nitrate, ammonium, and iron throughout the water column, all of which can impact primary production by the phytoplankton. Silicon is presently not taken into account, as it is thought to be non-limiting in our region of interest (C. Mordy, Pers. Comm.). Limitation of nitrate uptake by ammonium follows the Lomas and Glibert (1999) formulation that prevents the complete limitation of nitrate uptake even at high ammonium concentrations. Ammonium uptake is constrained to ensure that $Lim_{NO3}+Lim_{NH_4}\leq1$ (see Table 2 for details). The model has two size classes of phytoplankton; 'large' are considered to represent the prevalent bloom forming diatoms >10 μm, and 'small' represent a mixed assemblage of smaller cells. The two phytoplankton size classes can be differentiated by their maximum growth rates, response to nutrients and light, and availability to zooplankton grazers. Following Denman et al. (1998), it is assumed that at any given time phytoplankton growth is limited only by the most limiting factor (light, nutrients, temperature). Phytoplankton mortality due to senescence is modeled with a simple linear rate, and phytoplankton respiration is incorporated following Arhonditsis and Brett (2005).

2.1.1.2. Microzooplankton. Despite the diversity of microzooplankton in the Bering Sea ecosystem (Strom and Fredrickson, 2008) BEST–BSIERP field scientists recommended that the microzooplankton in the model be represented by a single model component (E. Sherr and D. Stoecker, Pers. Comm.). This reflects the community's present lack of knowledge
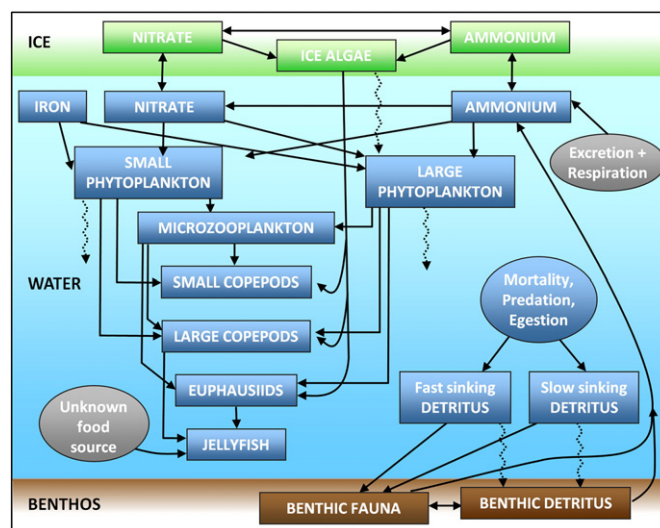
Fig. 1. Schematic illustration of the structure and direction of material flow in the BEST–NPZD model. The core pelagic model which has 12 state variables is coupled to an ice biology model with 3 state variables and to a benthic sub-model with 2 state variables. Arrows show the direction of material flow.

Table 1
Model equations for the *BEST–NPZD* model. For clarity advection and diffusion terms have been omitted. Sub equations are presented in Table 2.

State variable	Equation
Nitrate (NO_3)	$\frac{\partial NO_3}{\partial t} = -\xi\left(PS \cdot Pmax_{PS} \cdot \min(Lim_{LightPS}, Lim_{NO_3PS}, Lim_{FePS}) + PL \cdot Pmax_{PL} \cdot \min(Lim_{LightPL}, Lim_{NO_3PL}, Lim_{FePL})\right) + Nitrif$
Ammonium (NH_4)	$\frac{\partial NH_4}{\partial t} = -\xi\left(\begin{array}{l} PS \cdot Pmax_{PS} \cdot \min(Lim_{LightPS}, Lim_{NH_4PS}) \\ + PL \cdot Pmax_{PL} \cdot \min(Lim_{LightPL}, Lim_{NH_4PL}) \\ + Resp_{PS} + Resp_{PL} + Resp_{ZM} + Resp_{ZS} \\ + Resp_{ZL} + Resp_E + Resp_J + Resp_B \\ + Remin_D + \frac{1}{h_{z=1}}\left(Remin_{BD} \cdot f_{NO_2} + Defec_B\right) \end{array}\right) - Nitrif$
Iron (Fe)	$\frac{\partial Fe}{\partial t} = -\zeta\left(\begin{array}{l} PS \cdot Pmax_{PS} \cdot \min(Lim_{LightPS}, Lim_{NO_3PS}, Lim_{FePS}) \\ + PL \cdot Pmax_{PL} \cdot \min(Lim_{LightPL} \cdot Lim_{NO_3PL} \cdot Lim_{FePL}) \end{array}\right) + N_{Fe}(Fe - Fe_{clm})$
Small phytoplankton (PS)	$\frac{\partial PS}{\partial t} = PS \cdot Pmax_{PS} \cdot \left(\min(Lim_{LightPS}, Lim_{NO_3PS}, Lim_{FePS}) + \min(Lim_{LightPS}, Lim_{NH_4PS})\right)$ $\quad - Graz_{ZMPS} - Graz_{ZSPS} - Graz_{ZLPS} - Graz_{EPS} - Graz_{BPS} \cdot H_{Z=1}^{-1}$ $\quad - Resp_{PS} - Mort_{PS} - Sink_{PS}$
Large phytoplankton (PL)	$\frac{\partial PL}{\partial t} = PL \cdot Pmax_{PL} \cdot \left(\min(Lim_{LightPL}, Lim_{NO_3PL}, Lim_{FePL}) + \min(Lim_{LightPL}, Lim_{NH_4PL})\right)$ $\quad - Graz_{ZMPL} - Graz_{ZSPL} - Graz_{ZLPL} - Graz_{EPL} - Graz_{BPL} \cdot H_{Z=1}^{-1}$ $\quad - Resp_{PL} - Mort_{PL} - Sink_{PL}$
Ice algae (AI)	$\frac{\partial AI}{\partial t} = Grow_{AI} - Resp_{AI} - Graz_{AIZS} - Graz_{AIZL} - Graz_{AIE} - Mort_{AI} - Sink_{AI} - Flux_{AI}$
Microzooplankton (ZM)	$\frac{\partial ZM}{\partial t} = \gamma_{ZM} \cdot (Graz_{ZMPS} + Graz_{ZMPL}) - Graz_{ZSZM} - Graz_{ZLZM} - Graz_{EZM} - Resp_{ZM} - Pred_{ZM}$
Small copepods (ZS)	$\frac{\partial ZS}{\partial t} = \gamma_{ZS} \cdot (Graz_{ZSPS} + Graz_{ZSPL} + Graz_{ZSZM}) - Graz_{ZLZS} - Graz_{EZS} - Graz_{JZS} - Resp_{ZS} - Pred_{ZS}$
Large copepods (ZL)	$\frac{\partial ZL}{\partial t} = \gamma_{ZL} \cdot (Graz_{ZLPS} + Graz_{ZLPL} + Graz_{ZLZM}) - Graz_{ZLJ} - Resp_{ZL} - Pred_{ZL}$
Euphausiids (E)	$\frac{\partial E}{\partial t} = \gamma_E \cdot (Graz_{EPS} + Graz_{EPL} + Graz_{EZM} + Graz_{EZS}) - Resp_E - Molt_E - Mort_E - Pred_{EJ}$
Jellyfish (J)	$\frac{\partial J}{\partial t} = \gamma_J \cdot (Graz_{JZS} + Graz_{JZL} + Graz_{JE}) - Resp_J - Pred_J$
Benthic infauna (B)	$\frac{\partial B}{\partial t} = Graz_{BPS} + Graz_{BPL} + Graz_{BD} + Graz_{BDF} - Resp_B - Mort_B - Pred_B - Defec_B$
Benthic detritus (BD)	$\frac{\partial BD}{\partial t} = Defec_B + Mort_{BD} + Pred_{BD} + (Sink_{PS}(z=h) + Sink_{PL}(z=h) + Sink_D(z=h) + Sink_{DF}(z=h)) \cdot Hz$ $\quad - Graz_{BBD} - Remin_{BD}$
Slow sinking detritus (D)	$\frac{\partial D}{\partial t} = (1 - \gamma_{ZM}) \cdot (Graz_{ZMPS} + Graz_{ZMPL}) + Mort_{PS} + Mort_{PL} + Pred_{ZM} - Graz_{DB} \cdot H_{Z=1}^{-1} - Remin_D - Sink_D$
Fast sinking detritus (DF)	$\frac{\partial DF}{\partial t} = (1 - \gamma_{ZS}) \cdot (Graz_{ZSPS} + Graz_{ZSPL} + Graz_{ZSZM}) + (1 - \gamma_{ZL}) \cdot (Graz_{ZLPS} + Graz_{ZLPL} + Graz_{ZLZM})$ $\quad + (1 - \gamma_E) \cdot (Graz_{EPS} + Graz_{EPL} + Graz_{EZM} + Graz_{EZS}) + \min(0, 1 - \gamma_J) \cdot (Graz_{JZS} + Graz_{JZL} + Graz_{JE})$ $\quad + Pred_{ZS} + Pred_{ZL} + Pred_E + Pred_J - Graz_{DFB} \cdot H_{Z=1}^{-1} - Remin_{DF} - Sink_{DF}$

on what size class of microzooplankton eats what size phytoplankton and the fact that all sizes of mesozooplankton appear to consume both large and small microzooplankton. This aggregated representation of microzooplankton in the model means that, in addition to senescence, there is a large amount of cannibalism occurring within this trophic level. These losses were represented by a quadratic 'mortality' term. Grazing was formulated following Ryabchenko et al. (1997), which is an extension of the Holling type III grazing function to multiple prey resources. Losses due to temperature-dependent respiration were incorporated following Arhonditsis and Brett (2005) but were assumed to be limited at low food concentrations.

2.1.1.3. Mesozooplankton. The *BEST–NPZD* model tracks the biomass of small copepods, large copepods, and euphausiids. As with microzooplankton, grazing for each of the mesozooplankton groups follows a Holling type III formulation adapted to multiple prey sources (Ryabchenko et al., 1997) and respiration losses were dependent on temperature and food availability. Small copepods graze on small and large phytoplankton and microzooplankton. Large copepods graze on small phytoplankton but have a preference for large phytoplankton and microzooplankton. With varying preference, euphausiids consume large phytoplankton, microzooplankton, and small copepods. All mesozooplankton groups are potentially eaten explicitly by jellyfish and implicitly by 'undefined

predators'. The undefined loss is represented by a quadratic closure term, and is directed into the fast sinking detritus.

2.1.1.4. Jellyfish. A 'jellyfish' component is included in the *BEST–NPZD* model because, at times, jellyfish comprise a substantial portion of zooplankton biomass on the Bering Sea shelf and can contribute significantly to grazing of calanoid copepods and euphausiids (Brodeur et al., 2002). In the model, jellyfish are parameterized to represent the hydromedusae *Chrysaora melanaster* that can constitute 80% of the overall gelatinous zooplankton biomass in the region (Brodeur et al., 2002). The jellyfish formulations are detailed in Tables 1 and 2. Measuring functional responses for jellyfish is difficult and compounded by problems in determining biomass of individuals, container effects, and experiment duration. Baseline parameters for the jellyfish equations (Table 3) were selected to give a summertime biomass and food ration within the range predicted by Brodeur et al. (2002).

Hansson and Kiørboe (2006) found that jellyfish that have been allowed to adjust to their food concentrations, as would be the case in the natural environment, exhibit a saturation feeding response to increasing prey concentration. As such, in the model, jellyfish ingestion is represented by a Hollings type III function similar to that used for the other zooplankton. Copepods and euphausiids constitute 40–85% of the prey items in the stomachs of individual *C. melanaster*. Other prey items

Table 2
Sub-equations for the BEST–NPZD model. Model parameters and their values are defined in Table 3.

Description	Sub-Equations
Photosynthetically available radiation	$PAR_z = PAR_{frac} \cdot I_0 \cdot \exp^{-z \cdot (k_w + k_{chl}^*)}$ where $k_{chl}^* = \begin{cases} k_{chl} \cdot (PS^* + PL^*)^{0.428}, & (PS^* + PL^*) > 1 \\ k_{chl}, & (PS^* + PL^*) \leq 1 \end{cases}$
Phytoplankton doubling rate	$D_{rateX} = Di_X(10)^{Dp_X \cdot T}$ where $X = PS$ or PL
Maximum carbon-specific photosynthetic rate	$Pmax_X = (2^{D_{rateX}} - 1)$ where $X = PS$ or PL
Maximum chl-a specific photosynthetic rate	$Pmax_X^* = ccr_X \cdot Pmax_X$ where $X = PS$ or PL
Light limitation	$Lim_{LightX} = \tanh\left(\dfrac{\alpha_X \cdot PAR_z}{Pmax_X^*}\right)$ where $X = PS$ or PL
Nitrate limitation	$Lim_{NO_3X} = \dfrac{NO_3}{k_{1X} + NO_3} \cdot \left(1 - 0.8 \cdot \dfrac{NH_4}{k_{2X} + NH_4}\right)$ where $X = PS$ or PL
Ammonium limitation	$Lim_{NH_4X} = \begin{cases} \dfrac{NH_4}{k_{2X} + NH_4}, & Lim_{NO_3X} + \dfrac{NH_4}{k_{2X} + NH_4} < 1 \\ 1 - Lim_{NO_3X}, & Lim_{NO_3X} + \dfrac{NH_4}{k_{2X} + NH_4} > 1 \end{cases}$ where $X = PS$ or PL
Iron limitation	$Lim_{FeX} = \dfrac{Fe}{k_{FeX} + Fe} \cdot \dfrac{k_{FeX} + 2}{2}$ where $X = PS$ or PL
Temperature function	$f_{TY} = Q_{10Y}^{\frac{T - Q_{10YT}}{10}}$ where $Y = ZM, ZS, ZL, E, J$ or B
Grazing by microzooplankton	$Graz_{ZMY} = \dfrac{e_{ZM} \cdot fp_{YZM} \cdot Y^2}{k_{ZM} + fp_{PSZM} \cdot PS^2 + fp_{PLZM} \cdot PL^2} \cdot ML \cdot f_{TZM}$ where $Y = PS$ or PL
Grazing by small copepods	$Graz_{ZSY} = \dfrac{e_{ZS} \cdot fp_{YZS} \cdot Y^2}{k_{ZS} + fp_{PSZS} \cdot PS^2 + fp_{PLZS} \cdot PL^2 + fp_{ZMZS} \cdot ZM^2} \cdot ZS \cdot f_{TZS}$ where $Y = PS, PL$ or ML
Grazing by large copepods	$Graz_{ZLY} = \dfrac{e_{ZL} \cdot fp_{YZL} \cdot Y^2}{k_{ZL} + fp_{PSZL} \cdot PS^2 + fp_{PLZL} \cdot PL^2 + fp_{ZMZL} \cdot ZM^2} \cdot ZL \cdot f_{TZL}$ where $Y = PS, PL$ or ZM
Grazing by euphausiids	$Graz_{EY} = \dfrac{e_E \cdot fp_{YE} \cdot Y}{k_E + fp_{PSE} \cdot PS^2 + fp_{PLE} \cdot PL^2 + fp_{ZME} \cdot ZM^2 + fp_{ZSE} \cdot ZS^2} \cdot E \cdot f_{TE}$ where $Y = PS, PL, ZM$ or ZS
Grazing by jellyfish	$Graz_{YJ} = \dfrac{fp_{YJ} \cdot Y^2}{k_J + fp_{ZSJ} \cdot ZS^2 + fp_{ZLJ} \cdot ZL^2 + fp_{EJ} \cdot E^2} \cdot e_J \cdot f_{TJ} \cdot J$ where $Y = ZS, ZL$ or E
Grazing by benthic infauna on pelagic food	$Graz_{BY} = e_B \cdot f_{TB} \cdot B \cdot F_Y \cdot \dfrac{1}{F + K_P^{up}}$ where $F_Y = \dfrac{fp_{YB} \cdot Y_{z=1}}{fp_{YB} \cdot Y_{z=1} + L_P^{up}} \cdot fp_{YB} \cdot Y_{z=1}$ $F = \sum_Y F_Y$ and Y is PS, PL, D or DF
Grazing by benthic infauna on benthic detritus	$Graz_{BBD} = e_B \cdot f_{TB} \cdot B \cdot F_{BD} \cdot \dfrac{1}{F_{BD} + K_B^{up}}$ where $F_{BD} = \dfrac{fp_{BDB} \cdot BD}{fp_{BDB} \cdot BD + L_B^{up}} \cdot fp_{BDB} \cdot BD$
Defecation by benthic infauna	$Defec_B = d_B \cdot Graz_{BBD} + d_B \cdot Graz_{BD} + d_B \cdot Graz_{BBD} + d_P \cdot Graz_{BDPS} + d_P \cdot Graz_{BDPL}$
Sinking rate	$Sink_X = (w_X)\dfrac{\partial X}{\partial z}$ where $X = PS, PL, D$ or DF
Phytoplankton respiration	$Resp_X = X \cdot bm_X \cdot e^{kt_X(T - T_{refX})}$ where $X = PS$ or PL
Zooplankton respiration	$Resp_Y = Y \cdot bm_Y \cdot e^{kt_Y(T - T_{refY})}$ $bm_Y = \begin{cases} bm_{Y0}, & F_Y \geq 0.01 \\ bm_{Y0} \cdot \dfrac{F_Y}{0.01}, & F_Y < 0.01 \end{cases}$ where F_Y is the concentration of available food for species Y and $Y = ZM, ZS, ZL, E$ or J
Benthic infauna respiration	$Resp_B = B \cdot bm_B \cdot f_{TB} + am_B \cdot \gamma_B \cdot F_B$
Phytoplankton mortality	$Mort_X = m_X \cdot X$ where $X = PS$ or PL
Zooplankton mortality	$Pred_Y = p_Y \cdot Y^2$ where Y is ZM, ZS, ZL, E or J
Benthic infauna mortality	$Mort_B = m_B \cdot f_{TB} \cdot B$
Undefined predation on benthic infauna	$Pred_B = m_B \cdot f_{TB} \cdot B^2$
Detrital remineralization	$Remin_X = V_{0D} \cdot e^{k_{V0} \cdot T} \cdot X \cdot \xi$ where $X = D, DF$ or BD
Nitrification	$Nitrif = n_{max} \cdot \exp^{-Kt_{Nitr}(T - T_{optNitr})^2} \cdot NH_4$

include juvenile pollock, gelatinous zooplankton, and crab larvae (Brodeur et al., 2002; Trites et al., 1999). To reflect this diet, in the model jellyfish can feed on an un-modeled food source in addition to the explicitly represented small- and large-bodied copepods and euphausiids. The additional food source is represented simplistically through

the assimilation efficiency parameter (γ_J). Assimilation efficiency parameters usually vary from 0 (no material assimilated) to 1 (all material assimilated). To provide jellyfish with additional prey γ_J was permitted to exceed 1 during the parameter selection process, thus invoking a carbon supply to the model. Losses from jellyfish due to

Table 3
BEST–NPZD parameter definitions and modal values. The minimum and maximum of the continuous triangular probability distributions used in Ex. III and Ex. IV are also shown. The minimum and maximum of the parameter distributions in Ex. I and Ex. II are not shown but were $\pm 10\%$ and $\pm 60\%$ of the mode respectively.

Parameter	Description	Units	Mode	Minimum	Maximum
PAR_{frac}	Fraction of photosynthetically available light	–	0.5	0.45	0.55
k_w	Seawater light extinction coefficient	m^{-1}	0.046	0.046	0.065
k_{chl}	Phytoplankton light extinction coefficient	m^{-1}	0.0518	0.045	0.08
ξ	Nitrogen:Carbon ratio	mmol N $(mg\,C)^{-1}$	0.0126	0.01194	0.02016
Small phytoplankton (PS)					
Di_{PS}	Doubling rate for PS	d^{-1}	0.5	0.1	1.4
Dp_{PS}	Doubling rate exponent for PS	–	0.0275	0.0275	0.0631
α_{PS}	Slope of P–I curve for PS	mg C $(mg\,chl\text{-}a)^{-1}\,Em^{-2}$	5	3.2	9.2
k_{FePS}	PS half-saturation constant for iron	$\mu mol\ Fe\ m^{-3}$	0.2	0.1	0.3
k_{1PS}	PS half-saturation constant for NO_3	mmol N m^{-3}	2	1.0	20.0
k_{2PS}	PS half-saturation constant for NH_4	mmol N m^{-3}	0.5	0.2	20.0
kt_{PS}	Temperature coefficient for PS respiration	°C	0.03	0.02	0.069
bm_{PS}	Basal metabolic rate for PS	d^{-1}	0.02	0.01	0.16
$Tref_{PS}$	Reference temperature for PS respiration	°C	10	10	10
m_{PS}	Daily linear mortality rate for PS	d^{-1}	0.01	0.01	0.1
w_{PS}	Sinking rate for PS	$m\ s^{-1}$	0.1	0.0	0.5
ccr_{PS}	Carbon:Chlorophyll-a ratio for PS	mg C $(mg\,Chl)^{-1}$	65	40	100
Large phytoplankton (PL)					
Di_{PL}	Doubling rate parameter for PL	d^{-1}	0.5	0.06	1.0
Dp_{PL}	Doubling rate exponent for PL	–	0.0275	0.0275	0.0631
α_{PL}	Slope of P–I curve for PL	mg C $(mg\,chl\text{-}a)^{-1}\,Em^{-2}$	2.0	0.83	4.4
k_{FePL}	PL half-saturation constant for iron	$\mu mol\ Fe\ m^{-3}$	1	0.75	1.25
k_{1PL}	PL half-saturation constant for NO_3	mmol N m^{-3}	1.0	0.5	5.0
k_{2PL}	PL half-saturation constant for NH_4	mmol N m^{-3}	0.75	1.0	5.0
kt_{PL}	Temperature coefficient for PL respiration	°C	0.03	0.02	0.069
$Tref_{PL}$	Reference temperature for PL respiration	°C	10	10	10
bm_{PL}	Basal metabolic rate for PL	d^{-1}	0.02	0.01	0.16
m_{PL}	Daily linear mortality rate for PL	d^{-1}	0.01	0.01	0.1
w_{PL}	Sinking rate for PL	$m\ s^{-1}$	1	1.0	10.0
ccr_{PL}	Carbon:Chlorophyll-a ratio for PL	mgC $(mg\,Chl)^{-1}$	25	20	50
Microzooplankton (ZM)					
e_{ZM}	ZM maximum specific ingestion rate	mg C $(mg\,C)^{-1}\,d^{-1}$	0.45	0.1	1.0
γ_{ZM}	Assimilation efficiency for ZM	–	0.7	0.5	1.0
Q_{10ZM}	Q_{10} for ZM growth rate	–	2	1.1	2.2
Q_{10ZMT}	Temperature coefficient for Q_{10ML}	°C	5	5.0	5.0
k_{ZM}	Half-saturation constant for ZM grazing	mg C m^{-3}	20	5	30
fp_{PSZM}	Feeding preference of ZM for PS	–	1	0.4	1.0
fp_{PLZM}	Feeding preference of ZM for PL	–	0.2	0.1	1.0
bm_{ZM}	Basal metabolic rate for ZM	d^{-1}	0.08	0.04	0.16
kt_{MZ}	Temperature coefficient for ZM respiration	°C	0.069	0.02	0.08
$Tref_{ZM}$	Reference temperature for ZM respiration	°C	8	8	8
p_{ZM}	Daily nonlinear mortality for ZM	d^{-1}	0.005	0.002	0.1
Small copepods (ZS)					
e_{ZS}	ZS maximum specific ingestion rate	mg C $(mg\,C)^{-1}\,d^{-1}$	0.4	0.08	0.7
γ_{ZS}	Assimilation efficiency for ZS	–	0.7	0.5	1.0
Q_{10ZS}	Q_{10} for ZS growth rate	–	1.7	1.1	2.22
Q_{10ZST}	Temperature coefficient for Q_{10ZS}	°C	5	4.5	5.5
k_{ZS}	Half-saturation constant for ZS grazing	mg C m^{-3}	30	12	48
fp_{PSZS}	Feeding preference of ZS for PS	–	0.5	0.3	1.0
fp_{PLZS}	Feeding preference of ZS for PL	–	1	0.5	1.0
fp_{ZMZS}	Feeding preference of ZS for ZM	–	1	0.5	1.0
bm_{ZS}	Basal metabolism reference for ZS	d^{-1}	0.04	0.002	0.08
kt_{ZS}	Temperature coefficient for ZS respiration	°C	0.05	0.02	0.08
$Tref_{ZS}$	Reference temperature for ZS respiration	°C	15	15	15
p_{ZS}	Daily nonlinear mortality for ZS	d^{-1}	0.05	0.004	0.0275
Large copepods (ZL)					
e_{ZL}	ZL maximum specific ingestion rate	mg C $(mg\,C)^{-1}\,d^{-1}$	0.3	0.06	0.5
γ_{ZL}	Assimilation efficiency for ZL	–	0.7	0.5	1.0
Q_{10ZL}	Q_{10} for ZL growth rate	–	1.6	1.1	2.2
Q_{10ZLT}	Temperature coefficient for Q_{10ZL}	°C	5	5.0	5.0
k_{ZL}	Half-saturation constant for ZL grazing	mg C m^{-3}	30	20	125
fp_{PSZL}	Feeding preference of ZL for PS	–	0.1	0.0	1.0
fp_{PLZL}	Feeding preference of ZL for PL	–	1	0.5	1.0
fp_{ZMZL}	Feeding preference of ZL for ZM	–	1	0.5	1.0
bm_{ZL}	Basal metabolism reference for ZL	d^{-1}	0.03	0.001	0.06
kt_{ZL}	Temperature coefficient for ZL respiration	°C	0.05	0.02	0.08
$Tref_{ZL}$	Reference temperature for ZL respiration	°C	5	5	5
p_{ZL}	Daily nonlinear mortality for ZL	d^{-1}	0.05	0.004	0.0275

Table 3 (continued)

Parameter	Description	Units	Mode	Minimum	Maximum
Euphausiids (E)					
e_E	E maximum specific ingestion rate	mg C (mg C)$^{-1}$ d^{-1}	0.3	0.03	0.3
γ_E	Assimilation efficiency for E	–	0.7	0.63	0.77
Q_{10E}	Q_{10} for E growth rate	–	1.5	1.1	2.2
Q_{10ET}	Temperature coefficient for Q_{10E}	°C	5	4.5	5.5
k_E	Half-saturation constant for E grazing	mg C m^{-3}	20	15	100
fp_{PSE}	Feeding preference of E for PS	–	1	0.5	1.0
fp_{PLE}	Feeding preference of E for PL	–	1	0.5	1.0
fp_{ZME}	Feeding preference of E for ZM	–	0.2	0.1	1.0
bm_E	Basal metabolism reference for E	d^{-1}	0.02	0.008	0.05
kt_E	Temperature coefficient for E respiration	°C	0.069	0.02	0.08
$Tref_E$	Reference temperature for E respiration	°C	5	5	5
p_E	Daily nonlinear mortality for E	d^{-1}	0.05	0.004	0.0275
Jellyfish (J)					
e_J	J maximum specific ingestion rate	mg C (mg C)$^{-1}$ d^{-1}	0.069	0.0276	0.1104
γ_J	Assimilation efficiency for J	–	1	0.8	2.0
Q_{10Je}	Q_{10} for J growth rate	–	2.4	2.0	3.0
Q_{10JTe}	Reference temperature for J growth	°C	10	10	10
Q_{10Jr}	Q_{10} for J resp rate	–	2.8	2.0	3.0
Q_{10JTr}	Reference temperature for J resp	°C	10	10	10
k_J	Half-saturation constant for J grazing	mg C m^{-3}	0.01	0.004	0.016
fp_{ZSJ}	Feeding preference of J for ZS	–	1	0.3	1.0
fp_{ZLJ}	Feeding preference of J for ZL	–	1	0.3	1.0
fp_{EJ}	Feeding preference of J for E	–	1	0.3	1.0
bm_J	Basal metabolism reference for J	d^{-1}	0.02	0.001	0.08
p_J	Daily nonlinear mortality for J	d^{-1}	0.006	0.0024	0.0096
Benthic infauna (BI)					
e_B	BI maximum specific ingestion rate	mg C (mg C)$^{-1}$ d^{-1}	0.1	0.032	0.128
d_P	Defecated fraction of live material	–	0.3	0.2	0.48
d_B	Defecated fraction of detrital material	–	0.5	0.5	0.80
Q_{10Be}	Q_{10} for BI growth rate	–	1.5	1.0	2.0
Q_{10Br}	Q_{10} for BI respiration	–	1.5	1.0	2.0
Q_{10TBe}	Reference temperature for BI growth	°C	5	5.0	5.0
Q_{10TBr}	Reference temperature for BI respiration	°C	5	5.0	5.0
fp_{PSB}	Feeding preference of BI for PS	–	0.1	0.3	1.0
fp_{PLB}	Feeding preference of BI for PL	–	0.1	0.3	1.0
fp_{DB}	Feeding preference of BI for detritus	–	1.0	1.0	1.0
bm_B	Basal metabolism reference for BI	d^{-1}	0.25	0.1	0.4
am_B	Active metabolism reference for BI	d^{-1}	0.0027	0.001	0.00432
L_B^{up}	Lower threshold for uptake of BD	mg C m^{-2}	292	116.88	467.2
L_P^{up}	Lower threshold for pelagic material uptake	mg C m^{-2}	1	0.9	1.1
K_B^{up}	Half-saturation constant for BI consuming BD	mg C m^{-2}	2000	0.0	3200
K_P^{up}	Half-saturation constant for BI consuming planktonic material	mg C m^{-2}	10	4	16
m_B	Daily linear mortality for BI	d^{-1}	1E−3	1E−4	2E−3
p_B	Daily nonlinear mortality for BI	d^{-1}	1E−7	9.0E−8	1.1E−7
Detritus (D and DF)					
w_{DS}	Slow sinking rate for D	m s^{-1}	1	1.0	10.0
w_{DF}	Fast sinking rate for D	m s^{-1}	10	10	40.0
V_{0D}	Decomposition rate of D and BD at 0 °C	d^{-1}	0.1	0.02	0.08
k_{V0}	Temperature coefficient for V_{0D}	°C^{-1}	0.03	0.0228	0.0912
f_{NO_2}	Fraction lost to nitrite gas	–	0.80	0.7	1.0
Nitrification					
n_{max}	Maximum rate of nitrification rate at 0 °C	d^{-1}	0.0107	0.004	0.0171
I_T	Threshold for light-inhibition of nitrification	W m^{-2}	0.0095	0.0038	0.0152
k_I	Half-saturation irradiance for nitrification	W m^{-2}	4	1.6	6.4
Kt_{Ntr}	Effect of temperature above and below T_{optNtr}	°C^{-2}	0.002	0.0008	0.0032
T_{optNtr}	Optimal temperature for nitrification	°C	28	28	28
k_{2Nit}	Half-saturation [NH_4] required for nitrification	mg N m^{-3}	0.057	0.0228	0.0912
Iron climatology					
Fe$_{InS}$	Inshore surface iron climatology	nM	2	1.8	3.2
Fe$_{InD}$	Inshore deep iron climatology	nM	2	1.8	3.2
Fe$_{Inh}$	inshore isobaths transition depth	m	200	0	800
Fe$_{OffS}$	Offshore surface iron climatology	nM	0.05	0.02	0.08
Fe$_{OffD}$	Offshore deep iron climatology	nM	0.6	0.24	0.96
Fe$_{Offh}$	offshore isobaths transition depth	m	500	0	800
ζ	Iron:Carbon ratio	nmol Fe (mg C)$^{-1}$	0.000167	0.0000667	0.0002667
Ice biology					
μ_0	Maximum growth rate of AI at 0 °C	d^{-1}	1.44	0.576	2.304
α_I	Chl-a specific attenuation coefficient for AI	W^{-1} m^{-2}	0.8	0.32	1.28
β_I	Photosynthetic efficiency of AI	W^{-1} m^{-2}	0.018	0.0072	0.0288
ψ	NH_4 inhibition of AI uptake of NO_3	(mmol N)$^{-1}$ m^3	1.46	1.0	3.0

Table 3 (continued)

Parameter	Description	Units	Mode	Minimum	Maximum
Ice biology					
k_{1AI}	AI half-saturation constant for NO_3	mol N m^{-3}	1	0.4	1.6
k_{2AI}	AI half-saturation constant for NH_4	mol N m^{-3}	4	1.6	6.4
r_{AI}	Respiration rate parameter for AI	d^{-1}	0.05	0.02	0.08
Rg_0	AI mortality rate at 0 °C	d^{-1}	0.022	0.0088	0.0352
Rg	Temperature coefficient	°C^{-1}	0.03	0.012	0.048
N_{Nit}	Nitrification factor for AI	d^{-1}	0.0149	0.00596	0.02384
Environment parameters					
P_{Ih}	Ice thickness parameter	–	See method text		
P_{It}	Ice timing parameter	days	See method text		
P_T	Temperature parameter	–	See method text		
P_S	Salinity parameter	–	See method text		
P_L	Light parameter	–	See method text		
Initial condition parameters					
P_N	Initial nitrate parameter	–	See method text		
P_0	Initial biomass for phytoplankton variables	mg C m^{-3}	1.0	0.1	20
Z_0	Initial biomass for zooplankton variables	mg C m^{-3}	0.1	0.001	1.0

respiration were simulated using a modified form of the temperature-dependent respiration relationship developed by Uye and Shimauchi (2005) for scyphomedusae species in Tokyo Bay. In the Bering Sea, jellyfish are a trophic dead end with cannibalism being the only form of predation (Pauly et al., 2009). To reflect the increased losses to cannibalism that would occur as jellyfish population size increases, we represent predation losses with a quadratic closure term.

2.1.1.5. Detritus. Detritus is represented by two state variables: 'fast sinking' and 'slow sinking'. Unassimilated food and deceased phytoplankton and microzooplankton become slow sinking detritus, while deceased mesozooplankton and waste products from meso-zooplankton become fast sinking detritus. Both detrital components undergo temperature-dependent re-mineralization to ammonium.

2.1.2. The benthic submodel

Benthic biogeochemical processes are explicitly represented through inclusion of a benthic submodel that comprises benthic infauna and benthic detritus. The benthic submodel is a single layer model with no vertical resolution. The height (h_z) of the bottom layer of the water column is used to determine the fluxes at the interface of the benthic and pelagic systems. Within the classification scheme for sediment–water exchange processes by Soetaert et al. (2000), this is considered a level 3 complexity. There is presently insufficient data to support the implementation of a more complex representation of the Bering Sea benthos.

Phytoplankton and detritus that sink out of the bottom layer of the water column can enter the benthic detritus. To represent the loss of bio-available material at the M2 study site due to processes that are not explicitly represented in the 1D model, i.e., burial and transportation off the shelf (Walsh et al., 1981; Walsh and McRoy, 1986) 20% of the sediment flux to the benthos is considered biologically unavailable and removed from the system. An additional 1% of the sediment flux to the benthos is assumed lost through de-nitrification, a process that is relatively small in the Bering Sea (D. Schull, Pers. Comm.).

The formulations used to simulate benthic infaunal processes are simplified versions of those used in the vertically explicit benthic biological submodel (Ebenhöh et al., 1995) of the European Regional Seas Ecosystem Model (ERSEM). The benthic infauna component in the BEST–NPZD model represents the dominant infauna groups in the Bering Sea that live wholly or partly within the sediment, i.e., bivalves, amphipods, and polychaetes (Coyle et al., 2007). This component is considered to consume benthic detritus (detritivore feeding mode) as well as a portion of detritus and phytoplankton from the bottom-most layer of the water column (suspension feeding mode). As in the ERSEM model (Ebenhöh et al., 1995) the infauna are able to exhibit 'preferences'

for the alternate prey fields (phytoplankton, detritus, benthic detritus), and uptake is temperature dependent. Defecation is calculated as a fraction of the uptake of each food source. The assimilation efficiency for benthic infauna consuming phytoplankton is greater than its assimilation efficiency when consuming pelagic or benthic detritus. This reflects the assumption that 'live' phytoplankton would have a higher nutritional content. Benthic infaunal respiration is separated into temperature-dependent basal respiration and active respiration dependent on the assimilation fluxes. Mortality of benthic infauna is assumed to be due to natural senescence (a linear loss term) and to predation by higher trophic levels (a quadratic closure term). This component is assumed to be sessile and impervious to the effects of advection, diffusion, or active migration.

2.1.3. Ice submodel

The ice submodel is a simple model, simulating nitrate, ammonium, and ice algae within the bottom 2 cm of the ice. It is a modification of the model by Jin et al. (2006). Notable differences are the exclusion of silicate limitation and the addition of water column mesozooplankton grazing on the ice algae. This addition reflects observations that in the eastern Bering Sea, both copepod and euphausiids can exhibit high grazing rates on ice algae (Campbell et al., 2010; Lessard et al., 2010).

2.1.4. The physical model

The BEST–NPZD model is fully coupled to the Regional Ocean Modeling System (ROMS). ROMS is a state-of-the-art, free-surface, hydrostatic, primitive equation ocean circulation model developed at Rutgers University and UCLA. Details of the ROMS model can be found in Haidvogel et al. (2008), Moore et al. (2004), and Shchepetkin and McWilliams (2005). CORE 2 (Large and Yeager, 2009) shortwave radiation, long-wave radiation, air pressure, air temperature, and humidity atmospheric products were used to force the coupled ROMS-NPZD model. However, water column temperature and salinity were nudged daily towards the climatological values derived for each run of the Monte Carlo simulation; see below for details. The coupled biophysical model was implemented in a 1D mode centered on the Bering Sea M2 mooring site (56.877°N, 164.057°W) in the middle shelf domain. The model grid has 42 vertical levels, which follow a stretched vertical coordinate system and has a bottom depth of 67 m.

2.2. Sensitivity analysis

We explored model sensitivity to biological parameter values, initial conditions, and physical forcing. Four separate Monte Carlo sensitivity analysis experiments were performed; they differed in the range from which the biological and environmental parameters were randomly

selected. A Latin Hypercube Sampling procedure (Megrey and Hinckley, 2001) was implemented to select the parameter values for each experiment. By dividing parameter space into sections and sampling from each section with a certain probability, this stratified sampling method ensured more even coverage of parameter space than pure random sampling.

2.2.1. Variability in biological parameters

Values for the 135 biological parameters were randomly selected from continuous triangular probability distributions; no correlations between parameters were assumed. The modal, or baseline, values (Table 3) for each parameter were our best estimates for the values based on literature reviews and on input from the *BEST–BSIERP* field scientists. In the first experiment (Ex. I), the upper and lower limits of the probability distributions were defined as ± 10% of the baseline values. In the second experiment (Ex. II), the limits of the biological parameter ranges were increased to ± 60% of the baseline values. In the third (Ex. III) and fourth (Ex. IV) experiments, the upper and lower limits of the parameter distributions were our 'best guess' of the minimum and maximum values guided by *BEST–BSIERP* field scientists and literature reviews. For those parameters whose range was essentially unknown, we assumed it to be ± 60% of the baseline value. Note, in the first two experiments (Ex. I and Ex. II), the probability distributions were always symmetric with the baseline values corresponding to the median values of the probability distributions. In the later two experiments (Ex. III and Ex. IV), the parameter probability distributions were not necessarily symmetric.

2.2.2. Variability in physical environment

Model sensitivity to a series of eight environmental parameters was explored. Five of these parameters were 'physical' parameters developed to explore variability in ice thickness (P_{Ih}) and timing (P_{It}), water temperature (P_T), salinity (P_S), and shortwave solar radiation (P_L). Three 'initial condition' parameters were used to explore variability in initial nitrate (N_0), initial phytoplankton (P_0), and initial zooplankton (Z_0) concentrations.

2.2.2.1. Ice. The time series of ice thickness for each model iteration was given by:

$$h_{ice(t)} = \overline{h}_{ice(t + P_{It})} + \sigma_{i(t + P_{It})} \cdot P_{Ih}, \tag{1}$$

where the time-dependent mean $\left(\overline{h}_{ice(t)}\right)$ and standard deviation ($\sigma_{i(t)}$) for ice thickness at the M2 site were calculated from the National Snow and Ice Data Center ice coverage data at the M2 mooring in an unusually cold year (1999) and an unusually warm year (2004). Following Jin et al. (2006), ice coverage measurements were converted to an estimate of ice thickness as:

$$h_{ice} = ice\,coverage * 1.2. \tag{2}$$

P_{It} was randomly selected from a triangular distribution with a mode of 0 and an upper and lower limit of ± 30 days. P_{Ih} had a minimum of − 0.7, a maximum of 1.0, and a mode of 0. The − 0.7 lower limit was selected to prevent the instance of negative ice thickness. For Ex. IV only, the upper limit was increased to 2.0.

2.2.2.2. Hydrology. Water column temperature and salinity were nudged with a daily timescale towards randomly generated salinity and temperature climatologies that were dependent on the environmental parameters P_T and P_S and calculated as follows:

$$T_{(z,t)} = \overline{T}_{z,t} + \sigma_{T(z,t)} \cdot P_T \tag{3}$$

$$S_{(z,t)} = \overline{S}_{(z,t)} + \sigma_{S(z,t)} \cdot P_S. \tag{4}$$

Mean temperature $\left(\overline{T}_{(z,t)}\right)$ and salinity $\left(\overline{S}_{(z,t)}\right)$ time and depth explicit profiles and associated standard deviations ($\sigma_{(z, t)}$) for the M2 mooring were derived from FOCI (http://www.pmel.noaa.gov/foci/) mooring and shipboard observations from 1999 and 2004. P_T and P_S were selected at random from triangular distributions with a mode of 0 and a minimum and maximum of − 0.7 and 1.0 for Ex. I–III, The − 0.7 minimum was selected to be consistent with the parameter range sampled for P_{Ih}. In Ex. IV the minimum and maximum were set at ± 2.0.

2.2.2.3. Light. The shortwave radiative forcing used for each model iteration was randomly generated as follows:

$$R_{(t)} = \overline{R}_{(t)} + \sigma_{R(t)} \cdot P_L, \tag{5}$$

where the time-dependent mean shortwave radiation $\overline{R}_{(t)}$ and associated standard deviation $\sigma_{R(t)}$ were determined from simulated downward shortwave radiation (CORE 2; Large and Yeager, 2009) for 1999–2004, and P_L was selected at random from a triangular distribution with a mode of 0 and a minimum and maximum of − 0.7 and 1.0 for Ex. I–III, and ± 2.0 for Ex. IV.

2.2.2.4. Initial conditions. The sensitivity of the model to the initial nitrate profile ($N_{0(z)}$) was determined by specifying the initial nitrate profile for each model simulation as follows:

$$N_{0(z)} = \overline{iNO}_{3(z)} + \sigma_{N(z)} \cdot P_N. \tag{6}$$

Mean depth dependent initial nitrate $\overline{iNO}_{3(z)}$ and standard deviation ($\sigma_{N(z)}$) were calculated from nitrate profiles taken in the vicinity of the M2 mooring before the onset of a phytoplankton bloom. March is typically the earliest month that this region is sampled due to seasonal ice cover. Profiles were considered for analysis if they were taken during March or April on the Bering Sea shelf in the vicinity of the M2 mooring, specifically, between 55°N and 58°N, eastward of 168°W, and in total water depths of 50–100 m. Profiles were included in the analysis only if the nitrate concentration at 10 m was ≥ 60% of the nitrate concentration at 40 m. This was assumed to indicate that a significant drawdown of nitrate, associated with the spring phytoplankton bloom, had not yet begun. A total of 139 profiles from five years and three projects (PROBES, 1979, 1980, 1981; Inner Front Project, 1999; BEST, 2007) met the specified criteria and were used in the calculation. The initial nitrate parameter P_N was selected randomly from a triangular distribution with a mode of 0 and a minimum and maximum of − 0.7 and 1.0 for Ex. I–III, and ± 2.0 for Ex. IV.

Due to harsh environmental conditions on the Bering Sea shelf in the winter, plankton sampling at the M2 station has been sparse; thus winter plankton biomass is poorly known. To explore model sensitivity to initial plankton conditions, initial phytoplankton concentrations (P_0) were selected at random from distributions with a mode of 1.0 and limits of 0.1 and 20 mg C m^{-3}, and initial zooplankton concentrations (Z_0) were selected at random from distributions with a mode of 0.1 and limits of 0.001 and 1 mg C m^{-3}. Initial plankton concentrations were assumed to be homogeneous throughout the water column.

2.2.3. Number of simulations

The sample size required for each Monte Carlo experiment was determined by examining the variance in three representative output variables, mean nitrate [NO_3], mean large phytoplankton [PL] and mean mesozooplankton [ZL]. Between 3000 and 4000 model simulations, the variance in each of the output variables ceased to show any notable decline. Therefore, each of the four Monte Carlo experiments (Ex. I–IV) comprised 3100 iterations of the coupled *ROMS-NPZD* model.

2.2.4. Parameter ranking

Following the approach by Verbeeck et al. (2006), an LSL multiple linear regression was performed to determine the regression co-efficients and rank the parameters in terms of their influence on the

model output variables. The uncertainties of each parameter were used as the independent variables for the regression equation, and the model outputs were the dependent variables. The regression coefficients (w_i) were estimated by minimizing the sum of square errors. These values were then used to calculate the overall variance ($\sigma_{\delta_y}^2$) in model output and the sensitivity coefficient (S_{v_i}) for each parameter, i.e.,

$$S_{v_i} = \frac{w_i^2 \cdot \sigma_{\delta_{v_i}}^2}{\sigma_{\delta_y}^2} \cdot 100\% \quad \text{where} \quad \sigma_{\delta_y}^2 \approx \sum_{i=1}^{n} w_i^2 \cdot \sigma_{\delta_{v_i}}^2 . \tag{7}$$

One of the key goals of the *BEST–BSIERP* modeling effort is to explore the linkages among climate, physical oceanography, and lower and upper trophic levels. We thus chose to explore the sensitivity of a broad range of model output variables including nutrients, plankton biomass, primary and secondary productivity, fluxes, and event timings. This broad look at model output provided a comprehensive picture of likely ecosystem behavior and flow of material up through the food web in the event of climate change. The 20 output variables considered were, annual mean nitrate $[NO_3]_{wc}$, phytoplankton $[P]_{wc}$ and zooplankton $[Z]_{wc}$, mean nitrate $[NO_3]_U$, ammonium $[NH_4]_U$, small phytoplankton $[PS]_U$, large phytoplankton $[PL]_U$, microzooplankton $[ZM]_U$, small copepods $[ZS]_U$, large copepods $[ZL]_U$, euphausiids $[E]_U$, and jellyfish $[J]_U$ averaged for the upper 40 m between May 1 and September 30, mean nitrate below 40 m between May 1 and September 30 $[NO_3]_B$, annual benthic infaunal biomass $[BI]$ and ice algae biomass $[PI]$, total primary productivity (*NPP*) and secondary productivity (*NSP*) in the upper 40 m, benthic productivity (*NBP*), the flux of organic material to the benthos (*SedFlux*), and the day that the phytoplankton first bloom (*BloomDay*), defined as the first day when total surface chlorophyll exceeds 5 μg l^{-1} (Whitledge, Pers. Comm.). Parameters were ranked according to the magnitude of their sensitivity parameter (S_{v_i}). Analysis of variance was performed to determine the percentage of variability in each model output variable that could be attributed to the top five and top ten ranked parameters compared with the variability that could be attributed to the physical and initial condition parameters.

3. Results

The sensitivity of ecosystem dynamics to physical forcing was dependent on the degree of variability permitted in the physical forcing relative to the degree of uncertainty in the biological parameters. When the biological parameters varied only a small amount ($\pm 10\%$) from their baseline values (i.e., close to our initial guess), the physical environment was important to the ecosystem behavior. All five physical parameters were ranked within the top ten for at least two output variables (Fig. 2a). The temperature (P_T) and light (P_L) parameters were the most far-reaching physical parameters, ranking within the top ten for 17 and 14 of the 20 examined output variables, respectively. Parameters controlling ice timing (P_{It}) and ice thickness (P_{Ih}) also had a broad reach, ranking in the top ten for at least a third of the output variables with occurrence scores of 7 and 8, respectively. The salinity parameter was highly ranked for only two variables, these were $[NH_4]_U$ and *BloomDay*. As salinity does not have a direct influence on either of these variables, this is presumably due to its influence on vertical mixing of the water column. The ice thickness parameter (P_{Ih}) ranked highly for both $[PS]_U$ and $[PL]_U$ (Table 4). However, when the two size classes of phytoplankton were considered collectively and integrated over the water column ($[P]_{wc}$), the temperature parameter (P_T) was the most influential physical parameter. Conversely, while P_T ranked within the top five for the individual zooplankton variables $[ZM]_U$, $[ZS]_U$, and $[E]_U$, no physical parameter ranked in the top five for mesozooplankton as a collective group integrated over the water column ($[Z]_{wc}$). Ice thickness (P_{Ih}) and light (P_L) were relatively important to bloom timing (*BloomDay*), but only P_L ranked highly for net primary productivity (*NPP*), sediment flux

(*SedFlux*), and benthic productivity (*NBP*). No physical parameters were highly ranked for net secondary productivity (*NSP*).

In Ex. II, where the relatively small variability in the physical parameters was maintained while biological parameter uncertainty was increased to within $\pm 60\%$ of baseline values, there was a notable decline in the reach and ranking of the physical parameters (Fig. 2b). Occurrence scores for P_T and P_{It} were reduced to 2 and 1, respectively, and P_L, P_{Ih}, and P_S had occurrence scores of zero. This indicated that the ecosystem dynamics was now controlled primarily by the biology parameters. Implementing our 'best guess' to describe the range of uncertainty in each biological parameter while retaining a relatively small variation in the physical environment (Ex. III) generally gave no change to the ranking of physical parameters relative to Ex. II; biological parameter uncertainty continued to dominate ecosystem dynamics (Fig. 2c and Table 4). The exception was the emergence of the temperature parameter (P_T) as relatively important to *BloomDay*.

In Ex. IV, the physical parameters were allowed to vary within a larger range ($\sigma_X = \pm 2.0$), more representative of environmental change, while uncertainty in biology parameter values was described by our 'best guess' for each parameter range. This experiment gave a different, and likely more accurate, picture of the importance of physical forcing to ecosystem dynamics. Some physical parameters were found to play a significant role in ecosystem dynamics, ranking highly for several output variables, despite the increased uncertainty in many of the biological parameters. For example, the ice timing (P_{It}), temperature (P_T), and light (P_L) parameters had occurrence scores of 5, 6, and 11, respectively (Fig. 2d). Ice thickness (P_{Ih}) and salinity (P_S) parameters have scores of zero, indicating their lesser role in controlling ecosystem dynamics at the study site.

The relative importance of biological initial conditions to model output was also dependent on the degree of uncertainty assumed for the biological parameters. When biological parameters were varied within a range close to their baseline values (Ex. I), parameters controlling initial phytoplankton (P_0) and initial nitrate (P_N) concentration ranked within the top ten for twelve of the output variables, while Z_0 was highly ranked for only a single output variable (Fig. 2a). A change in biological parameter uncertainty to $\pm 60\%$ (Ex. II) or to our 'best guess' (Ex. III) caused a notable decline in the influence of the initial conditions to overall ecosystem dynamics (Fig. 2b and c). In Ex. II, neither phytoplankton (P_0) nor zooplankton (Z_0) initial conditions were important to system dynamics, and the initial nitrate parameter (P_N) ranked within the top ten for only six output variables. Similarly, in Ex. III, the occurrence scores for Z_0, P_0, and P_N were 0, 1, and 5, respectively. In Ex. IV, the minimum and maximum range for P_N was increased to ± 2.0 and this parameter is seen to have a very broad reach, ranking within the top ten for 19 of the 20 output variables examined (Fig. 2d).

The top five (*Top5*) ranked parameters for each of the output variables (Table 4) accounted for between 32 and 89% of the variability in the output variables (Table 5) when physical variability and biological uncertainty were small (Ex. I). There was no clear pattern in the direction of the R^2 for the top five ranked parameters as the biological and the physical parameter ranges were varied (Ex. II–IV). In general, each of the physical parameters accounted for only a small percentage of the variability in each of the output variables, the R^2 being <0.01 in most cases. In Ex. I, temperature (P_T) did account for >5% of the variability in a number of the output variables, but its explanatory power was reduced to <1% when the biological parameters were selected from an expanded range of possibilities (Ex. II–IV). Across experiments, the parameter controlling initial nitrate concentration (P_N) had some of the highest R^2 values and, in addition to explaining a large percentage of the variability in the nutrient variables ($[NO_3]_U$, $[NH_4]_U$, $[NO_3]_B$, and $[NO_3]_{wc}$), explained 7% of the variability in primary productivity (*NPP*) in Ex. I and Ex. IV. Initial plankton biomass ($P_0 + Z_0$) could explain up to 14% of the variability in the output variables when biological and physical parameters were varied only within a narrow range (Ex. I), but their influence on ecosystem dynamics was reduced once the biological and
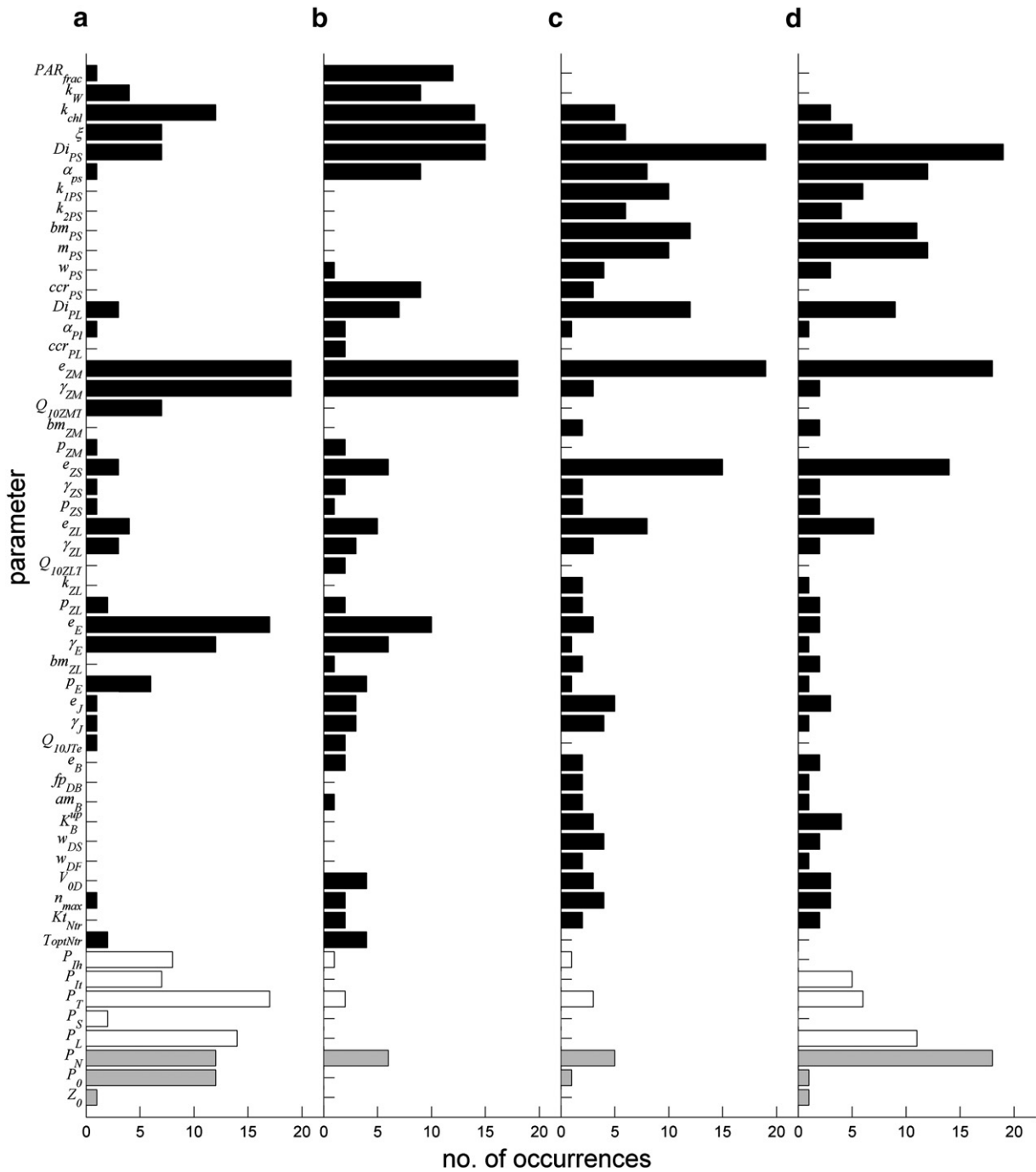
Fig. 2. Number of times a parameter ranked within the top ten for the twenty output variables considered for a) Ex. I, b) Ex. II, c) Ex. III and d) Ex. IV. For clarity, only parameters that ranked within the top ten for at least two variables in at least one of the experiments are shown. Black bars indicate biological model parameters, white bars indicate environmental parameters and gray bars indicate initial condition parameters. Parameter definitions and value ranges are presented in Table 3.

physical parameter ranges were expanded (Ex. II–IV). Initial plankton concentrations had the largest influence on nitrate ($[NO_3]_U$, $[NO_3]_B$, $[NO_3]_{wc}$) and *BloomDay*.

Of the 135 biological parameters explored, 71 ranked in the top 10 for at least one of the output variables during one of the experiments. Often a parameter was important only to its corresponding variable (Table 4). For example, the grazing rate (e_J) and assimilation efficiency (γ_J) of jellyfish ranked within the top five only for the output variable ($[J]_U$). However, there were several biological parameters that were consistently very important to a number of the output variables across experiments (Table 4). Microzooplankton grazing rate (e_{ZM}), for

example, was a top five ranked parameter for more than half of the output variables examined. The biological parameters γ_E, e_E, γ_{ZM}, e_{ZM}, and k_{chl} had the most far-reaching influence when biological parameter uncertainty was small (Ex. I, Fig. 2a). All these parameters remained important as parameter uncertainty increased (Ex II), and were joined by several other biological parameters. Notably, parameters controlling light availability in the system (PAR_{frac} and k_w), parameters controlling the growth of small phytoplankton (ccr_{PS}, α_{PS} and Di_{PS}), and the C:N ratio (ξ) had an increased role in controlling ecosystem dynamics. Moving from a fixed range for biological parameter uncertainty to our 'best guess' at the range for each parameter (Ex. III and Ex. IV) resulted in a

Table 4
Top five (Top5) ranked parameters for the twenty output variables considered for each of the four sensitivity experiment (Ex. I–V); See method text for description of experiments. Light gray shading indicated parameters that explained between 10 and 20% of output variance. Dark gray shading indicates parameters that explained >20% of output variance.

$[NO_3]_{wc}$

	I	II	III	IV
1st	P_N	k_{chl}	Di_{PS}	P_N
2nd	e_{ZM}	e_{ZM}	P_N	Di_{PS}
3rd	γ_{ZM}	Di_{PS}	e_{ZM}	e_{ZM}
4th	P_0	γ_{ZM}	e_{ZS}	P_{lh}
5th	P_{lh}	PAR_{frac}	k_{1PS}	P_L

$[P]_{wc}$

	I	II	III	IV
1st	e_{ZM}	ξ	e_{ZM}	e_{ZM}
2nd	γ_{ZM}	e_{ZM}	Di_{PS}	Di_{PS}
3rd	e_E	γ_{ZM}	m_{PS}	m_{PS}
4th	P_T	e_E	e_{ZS}	e_{ZS}
5th	P_{lh}	Di_{PS}	bm_{PS}	P_N

$[Z]_{wc}$

	I	II	III	IV
1st	e_{ZM}	γ_{ZL}	e_{ZL}	e_{ZL}
2nd	γ_{ZM}	e_{ZL}	e_{ZS}	e_{ZS}
3rd	e_E	m_{ZL}	m_{ZL}	Di_{PS}
4th	γ_{ZL}	e_{ZM}	Di_{PS}	m_{ZL}
5th	e_{ZL}	γ_{ZM}	e_{ZM}	e_{ZM}

BloomDay

	I	II	III	IV
1st	P_0	e_{ZM}	Di_{PS}	Di_{PS}
2nd	e_{ZM}	Di_{PS}	Di_{PL}	P_T
3rd	γ_{ZM}	k_{chl}	P_T	Di_{PL}
4th	P_{lh}	γ_{ZL}	k_{1PS}	k_{1PS}
5th	P_L	PAR_{frac}	k_{2PS}	P_L

SedFlux

	I	II	III	IV
1st	e_{ZM}	ξ	Di_{PS}	Di_{PS}
2nd	γ_{ZM}	k_{chl}	e_{ZM}	e_{ZM}
3rd	P_N	e_{ZM}	Di_{PL}	P_N
4th	P_L	PAR_{frac}	ξ	Di_{PL}
5th	k_{chl}	Di_{PL}	bm_{PS}	P_L

NPP

	I	II	III	IV
1st	e_{ZM}	ξ	Di_{PS}	Di_{PS}
2nd	γ_{ZM}	k_{chl}	e_{ZM}	P_N
3rd	P_N	PAR_{frac}	bm_{PS}	e_{ZM}
4th	e_E	Di_{PS}	α_{PS}	α_{PS}
5th	P_L	k_w	ξ	bm_{PS}

NSP

	I	II	III	IV
1st	e_{ZM}	γ_{ZL}	e_{ZM}	Di_{PS}
2nd	e_E	γ_{ZS}	Di_{PS}	e_{ZM}
3rd	γ_{ZM}	e_{ZL}	m_{PS}	m_{PS}
4th	γ_E	e_{ZM}	γ_{ZS}	γ_{ZS}
5th	m_E	e_{ZS}	e_{ZS}	P_N

NBP

	I	II	III	IV
1st	e_{ZM}	e_{ZM}	K_B^{up}	K_B^{up}
2nd	γ_{ZM}	k_{chl}	Di_{PS}	Di_{PS}
3rd	e_E	ξ	e_B	e_{ZM}
4th	k_{chl}	e_B	e_{ZM}	e_B
5th	P_L	γ_{ZM}	V_{0D}	α_{PS}

$[BI]$

	I	II	III	IV
1st	e_{ZM}	k_{chl}	K_B^{up}	Di_{PS}
2nd	γ_{ZM}	e_{ZM}	Di_{PS}	K_B^{up}
3rd	P_0	d_{Bb}	bm_B	bm_B
4th	P_T	PAR_{frac}	e_B	e_B
5th	P_{lh}	e_B	d_B	d_B

$[PI]$

	I	II	III	IV
1st	P_N	ξ	μ_0	P_{lh}
2nd	ξ	μ_0	ξ	μ_0
3rd	μ_0	N_0	ψ	N_0
4th	P_T	α_{PI}	α_{PI}	ξ
5th	P_0	k_{2PI}	P_N	P_T

$[PS]_U$

	I	II	III	IV
1st	e_{ZM}	ξ	Di_{PS}	Di_{PS}
2nd	e_E	e_{ZM}	e_{ZM}	e_{ZM}
3rd	P_{lh}	γ_{ZM}	m_{PS}	m_{PS}
4th	γ_{ZM}	e_E	Di_{PL}	Di_{PL}
5th	Di_{PL}	Di_{PL}	e_{ZS}	N_0

$[PL]_U$

	I	II	III	IV
1st	P_{lh}	Di_{PL}	Di_{PL}	Di_{PL}
2nd	Di_{PL}	ξ	w_{PL}	w_{PL}
3rd	P_N	Di_{PS}	Di_{PS}	Di_{PS}
4th	e_E	α_{PL}	e_{ZM}	α_{PL}
5th	Di_{PS}	e_E	α_{PL}	e_{ZM}

$[ZM]_U$

	I	II	III	IV
1st	P_N	γ_{ZM}	e_{ZM}	e_{ZM}
2nd	P_T	e_{ZM}	e_{ZS}	Di_{PS}
3rd	γ_{ZM}	e_E	Di_{PS}	e_{ZS}
4th	ξ	ξ	γ_{ZM}	γ_{ZM}
5th	e_E	m_{ZL}	bm_{ZM}	bm_{ZM}

$[ZS]_U$

	I	II	III	IV
1st	e_{ZM}	γ_{ZS}	e_{ZS}	e_{ZS}
2nd	γ_{ZM}	e_{ZS}	m_{ZS}	m_{ZS}
3rd	γ_{ZS}	m_{ZS}	γ_{ZS}	γ_{ZS}
4th	e_{ZS}	e_{ZM}	Di_{PS}	Di_{PS}
5th	P_T	γ_{ZM}	e_{ZM}	e_{ZM}

$[ZL]_U$

	I	II	III	IV
1st	e_{ZM}	γ_{ZL}	e_{ZL}	e_{ZL}
2nd	γ_{ZM}	e_{ZL}	m_{ZL}	m_{ZL}
3rd	γ_{ZL}	m_{ZL}	e_{ZS}	e_{ZS}
4th	e_E	e_{ZM}	γ_{ZL}	Di_{PS}
5th	e_{ZL}	γ_{ZM}	Di_{PS}	γ_{ZL}

$[E]_U$

	I	II	III	IV
1st	e_E	γ_E	e_E	e_E
2nd	γ_E	m_E	m_E	Di_{PL}
3rd	m_E	e_E	γ_E	bm_E
4th	e_{ZM}	ξ	Di_{PL}	γ_E
5th	P_T	γ_{ZM}	bm_E	m_E

$[J]_U$

	I	II	III	IV
1st	γ_J	γ_J	γ_J	γ_J
2nd	e_J	e_J	e_J	e_J
3rd	P_T	Q_{10TJe}	bm_J	bm_J
4th	Q_{10TJe}	Q_{10J}	e_{ZM}	P_T
5th	Q_{10J}	Q_{10TJr}	P_T	e_{ZM}

$[NO_3]_U$

	I	II	III	IV
1st	P_N	e_{ZM}	Di_{PS}	Di_{PS}
2nd	e_{ZM}	k_{chl}	e_{ZM}	P_N
3rd	γ_{ZM}	Di_{PS}	P_N	P_N
4th	P_0	γ_{ZM}	e_{ZS}	k_{1PS}
5th	e_E	PAR_{frac}	k_{1PS}	P_{lh}

$[NH_4]_U$

	I	II	III	IV
1st	P_N	T_{optNtr}	Di_{PS}	Di_{PS}
2nd	P_T	e_{ZM}	n_{max}	P_N
3rd	e_{ZM}	k_{chl}	w_D	n_{max}
4th	T_{optNtr}	n_{max}	V_{0D}	V_{0D}
5th	e_E	γ_{ZM}	Kt_{Ntr}	Kt_{Ntr}

$[NO_3]_B$

	I	II	III	IV
1st	P_N	k_{chl}	Di_{PS}	P_N
2nd	P_0	e_{ZM}	P_N	Di_{PS}
3rd	e_{ZM}	Di_{PS}	e_{ZM}	P_{lh}
4th	γ_{ZM}	PAR_{frac}	n_{max}	α_{PS}
5th	P_{lh}	γ_{ZM}	α_{PS}	Kt_{Ntr}

shift in the pattern of important parameters. e_{ZM}, α_{PS}, and Di_{PS} remained important biological parameters, but previously unimportant m_{PS}, e_{ZL}, e_{ZS}, bm_{PS}, Di_{PL}, k_{1PS}, and k_{2PS} had relatively high occurrence scores, while k_w and f_{PAR} were no longer important (Fig. 2c,d).

The range of simulated spring bloom timing (BloomDay) agrees well with the observed March–June timing of the spring bloom on the southern Bering Sea shelf (Fig. 3). In Ex. I, when biological parameter uncertainty was assumed small (± 10% of the baseline), BloomDay had a median of 109 (April 19) and a lower and upper fence of 100–119 (April 10–29). The median BloomDay was not affected by increasing the limits of the parameter ranges to ±60% (Ex. II), but there was an increased variability in timing. While the middle 50% of the estimates fall between days 94–122 (April 4–May 2) the lower and upper fence extend to 52 (Feb 21) and 164 (June 13) respectively. Adjusting the biological parameter ranges to our 'best guess' for each model parameter (Ex. III) resulted in a delay of almost 3 weeks in the median BloomDay (May 8) with an inter-quartile range of 116–143 (April 26–May 23). Very similar results were observed for EX. IV, indicating that the additional variability in the environmental variables did not create significant additional variability in bloom timing. BloomDay decreases (earlier bloom) with an increase in the light and temperature (Fig. 4a and b) and with a decrease in the ice thickness (Fig. 4c and d). The relationship between BloomDay and the ice timing parameter P_{It} is less straightforward, reflecting the complex climatological ice coverage at the M2 mooring site with intermittent periods of ice coverage and open water throughout the winter and spring. As P_{It} increased from −30 to +30 days, the BloomDay transitioned from very early to late to average. These trends were apparent in both Ex. I and Ex. IV.

The model's ability to simulate net primary productivity accurately (Fig. 5) varied with biological parameter uncertainty. Simulated net primary productivity (NPP) in Ex. I. had a median of 145.7 g C m^{-2} y^{-1} with a lower and upper fence of 96.3–211.6 g C m^{-2} y^{-1}, which agrees very well with the observed range of primary productivity on the Bering Sea shelf (145.7 ± 81.8 g C m^{-2} y^{-1}; Rho and Whitledge, 2007). Increasing biological uncertainty to ±60% of baseline values (Ex. II) reduced the median simulated productivity slightly to 139.9 g C m^{-2} y^{-1} but increased the variability. The lower and upper fence (9.7 and 305.4 g C m^{-2} y^{-1}, respectively) were outside the bounds of observations, but the inter-quartile range (104.8–185.2 g C m^{-2} y^{-1}) was well within the observed range. Expanding the biological parameter range to our 'best guess' (Ex. III and Ex. IV) resulted in median productivities of 58.4 and 56.2 g C m^{-2} y^{-1}, respectively. In these experiments the upper fence for NPP was 132.6 and 142.7 respectively, which is below the observed mean. This indicates that many of the parameter combinations used in these experiments are likely invalid for the Bering Sea ecosystem. The scatter plots in Fig. 6 show that in the case on small biological and physical uncertainty (EX. I) and with our 'best guess' for the parameter ranges (Ex. IV) NPP was not strongly correlated with the temperature parameter

Table 5

R^2 values to indicate the variability in the twenty output diagnostics that can be accounted for by variability in the top five ranked parameters (*Top5*, see Table 4), the environmental parameters for temperature (P_T), ice thickness (P_{Ih}) and light (P_L) and the initial condition parameters for nitrate (P_N) and plankton ($P_0 + Z_0$) for each of the four sensitivity experiment (Ex. I–IV). See method text for description of experiments. R^2 values exceeding 0.05 are shaded gray.

	$[NO_3]_{wc}$				$[P]_{wc}$				$[Z]_{wc}$				BloomDay			
	I	II	III	IV	I	II	III	IV	I	II	III	IV	I	II	III	IV
Top5	0.55	0.49	0.57	0.63	0.51	0.48	0.47	0.45	0.54	0.61	0.45	0.42	0.33	0.31	0.41	0.44
P_T	0.04	<0.01	<0.01	<0.01	0.05	<0.01	<0.01	<0.01	0.05	<0.01	<0.01	<0.01	<0.01	<0.01	0.02	0.09
P_{Ih}	0.07	<0.01	<0.01	0.03	0.07	<0.01	<0.01	<0.01	0.01	<0.01	<0.01	<0.01	0.03	<0.01	<0.01	0.01
P_L	0.03	0.01	<0.01	0.02	<0.01	<0.01	<0.01	<0.01	0.01	<0.01	<0.01	<0.01	0.03	0.01	<0.01	0.02
P_N	0.25	0.04	0.08	0.29	0.01	0.01	<0.01	0.03	0.01	<0.01	<0.01	0.01	<0.01	<0.01	<0.01	<0.01
$P_0 + Z_0$	0.08	<0.01	<0.01	<0.01	0.02	<0.01	<0.01	<0.01	<0.01	<0.01	<0.01	0.01	0.14	<0.01	<0.01	<0.01

	SedFlux				NPP				NSP				NBP			
	I	II	III	IV	I	II	III	IV	I	II	III	IV	I	II	III	IV
Top5	0.49	0.51	0.47	0.42	0.43	0.57	0.49	0.46	0.58	0.37	0.38	0.35	0.48	0.34	0.17	0.17
P_T	0.01	<0.01	<0.01	0.01	<0.01	<0.01	<0.01	0.01	0.01	<0.01	0.01	0.01	0.02	<0.01	<0.01	<0.01
P_{Ih}	0.01	<0.01	<0.01	<0.01	0.04	<0.01	<0.01	<0.01	0.02	<0.01	<0.01	<0.01	0.04	<0.01	<0.01	<0.01
P_L	0.07	<0.01	<0.01	0.03	0.04	<0.01	<0.01	0.02	0.01	<0.01	<0.01	0.02	0.03	<0.01	<0.01	<0.01
P_N	0.08	0.01	<0.01	0.08	0.07	0.02	0.02	0.07	0.01	0.01	0.01	0.03	0.01	<0.01	<0.01	0.01
$P_0 + Z_0$	<0.01	<0.01	<0.01	<0.01	0.01	<0.01	<0.01	<0.01	<0.01	<0.01	<0.01	<0.01	0.02	<0.01	<0.01	<0.01

	$[BI]$				$[PI]$				$[PS]_U$				$[PL]_U$			
	I	II	III	IV	I	II	III	IV	I	II	III	IV	I	II	III	IV
Top5	0.36	0.32	0.32	0.27	0.36	0.68	0.66	0.38	0.47	0.42	0.46	0.44	0.41	0.41	0.40	0.38
P_T	0.05	<0.01	<0.01	<0.01	0.04	0.01	0.01	0.01	0.04	<0.01	<0.01	<0.01	<0.01	<0.01	<0.01	0.01
P_{Ih}	0.08	<0.01	<0.01	<0.01	0.01	<0.01	0.01	<0.01	0.12	<0.01	<0.01	<0.01	0.19	<0.01	<0.01	<0.01
P_L	0.04	<0.01	<0.01	0.01	<0.01	<0.01	<0.01	0.01	<0.01	<0.01	<0.01	<0.01	0.02	<0.01	<0.01	0.01
P_N	0.01	<0.01	<0.01	0.02	0.18	0.03	0.02	0.01	0.01	0.01	0.01	0.03	0.04	0.01	<0.01	0.01
$P_0 + Z_0$	0.06	<0.01	<0.01	<0.01	0.01	<0.01	<0.01	<0.01	0.02	<0.01	<0.01	<0.01	0.03	<0.01	<0.01	<0.01

	$[ZM]_U$				$[ZS]_U$				$[ZL]_U$				$[E]_U$			
	I	II	III	IV	I	II	III	IV	I	II	III	IV	I	II	III	IV
Top5	0.32	0.43	0.45	0.41	0.55	0.69	0.57	0.55	0.52	0.66	0.51	0.48	0.62	0.59	0.50	0.41
P_T	0.07	<0.01	<0.01	<0.01	0.07	<0.01	<0.01	<0.01	0.06	<0.01	<0.01	<0.01	0.08	<0.01	<0.01	<0.01
P_{Ih}	<0.01	<0.01	0.01	<0.01	0.02	<0.01	<0.01	<0.01	0.02	<0.01	<0.01	<0.01	0.01	<0.01	<0.01	0.01
P_L	0.01	<0.01	<0.01	<0.01	<0.01	<0.01	<0.01	0.01	<0.01	<0.01	<0.01	<0.01	<0.01	<0.01	<0.01	0.01
P_N	0.11	<0.01	<0.01	0.01	0.01	<0.01	<0.01	<0.01	0.01	<0.01	<0.01	0.02	0.01	<0.01	<0.01	0.01
$P_0 + Z_0$	<0.01	<0.01	<0.01	0.01	<0.01	<0.01	<0.01	<0.01	<0.01	<0.01	0.01	0.01	<0.01	<0.01	0.01	0.02

	$[J]_U$				$[NO_3]_U$				$[NH_4]_U$				$[NO_3]_B$			
	I	II	III	IV	I	II	III	IV	I	II	III	IV	I	II	III	IV
Top5	0.89	0.60	0.63	0.58	0.59	0.50	0.56	0.59	0.52	0.41	0.30	0.30	0.52	0.45	0.49	0.62
P_T	0.24	0.01	0.01	0.03	0.03	<0.01	<0.01	0.01	0.12	0.01	<0.01	0.02	0.04	<0.01	<0.01	<0.01
P_{Ih}	<0.01	<0.01	<0.01	<0.01	0.04	0.01	<0.01	0.02	<0.01	<0.01	<0.01	<0.01	0.08	<0.01	0.01	0.04
P_L	<0.01	<0.01	<0.01	<0.01	0.04	<0.01	<0.01	0.02	0.01	<0.01	<0.01	<0.01	0.02	0.01	<0.01	0.02
P_N	<0.01	<0.01	<0.01	<0.01	0.27	0.04	0.04	0.18	0.20	0.02	0.01	0.08	0.23	0.04	0.13	0.38
$P_0 + Z_0$	<0.01	<0.01	0.01	0.01	0.05	<0.01	<0.01	<0.01	<0.01	<0.01	<0.01	<0.01	0.09	<0.01	<0.01	<0.01

(P_T) but was positively correlated with the initial nitrate parameter (P_N). NPP was also positively correlated with the light parameter (P_L, not shown).

In general, secondary productivity (NSP) was strongly positively correlated with primary productivity (NPP) and negatively correlated with BloomDay (Fig. 7); however, there is a decline in NSP in the event of a very early bloom. Considered collectively, mesozooplankton (small and large copepods + euphausiids) productivity was not correlated to P_T, but the distribution of the secondary production between the zooplankton components did vary with P_T. The relative fraction of secondary production undertaken by the small zooplankton size classes (microzooplankton + small copepods) increases with P_T, while the relative fraction undertaken by large zooplankton (large copepods + euphausiids) shows a corresponding decrease (Fig. 8). This relationship held true whether parameter values were varied by only a small amount (Ex. I) or within the full range of likely values (Ex. IV). In Ex. I, an increasing P_T also gave rise to an increase in the contribution of the pelagic mesozooplankton (small and large copepods and euphausiids) to secondary production relative to the benthic infauna (Fig. 9a),

indicating a shift towards a more pelagic food web as temperature increase. No such relationship was observed in Ex. IV (Fig. 9b).

Both mesozooplankton productivity and biomass were dependent on the grazing rates of several of the zooplankton groups in the model (Table 4). Mesozooplankton biomass and productivity increased with grazing rates e_{ZL} and e_E and decreased with increasing e_{ZM}. However, an increase in e_{ZS} caused a decrease in the mesozooplankton biomass but an increase in the mesozooplankton productivity; this highlights the non-linear complexities that arise from the linkage of multiple trophic levels.

The LSL method in combination with Monte Carlo analysis allows us to determine uncertainty in the BEST–NPZD model outputs as a function of uncertainty in the parameter values. Uncertainty in mesozooplankton biomass estimates varies throughout the year (Fig. 10) and is generally much smaller ($\sigma = 1.03$–6.47 mg C m^{-3}) when parameter uncertainty is small and constant (Ex. I) compared to our 'best guess' (Ex. IV, $\sigma = 1.19$–13.73 mg C m^{-3}). In Ex. I the uncertainty in biomass estimates was at a maximum during November and December when the standard deviation exceeded 100% of the mean and was at a
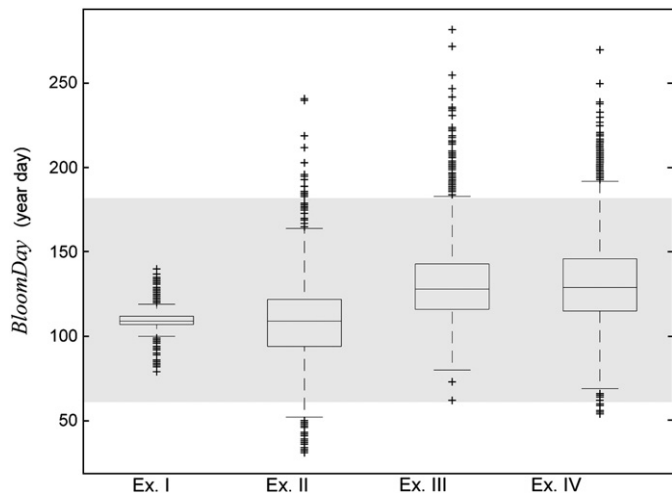
Fig. 3. Simulated variability in *BloomDay*, the first day of the spring phytoplankton bloom for Ex. I–IV. See method text for description of experiments. The gray shaded area shows the bounds of the observed spring bloom timing (Stabeno et al., 2001). On each box, the central mark is the median, the edges of the box are the 25th and 75th percentiles, the whiskers extend to the most extreme datum still within $1.5 \cdot IQR$ of the lower and upper quartiles. Suspected outliers are plotted individually (+).

Fig. 5. Simulated total annual primary production (*NPP*) in g C m^{-2} y^{-1} for each of the four sensitivity experiments, Ex. I–IV. See method text for description of experiments. The observed mean (thick black line) and 95% confidence interval (upper and lower bounds of the gray shaded area) for primary production on the Bering Sea shelf (Rho and Whitledge, 2007) are also shown. On each box, the central mark is the median, the edges of the box are the 25th and 75th percentiles, the whiskers extend to the most extreme datum still within $1.5 \cdot IQR$ of the lower and upper quartiles. Suspected outliers are plotted individually (+).

minimum from mid April through September when the standard deviation was less than 20% of the mean. Using the 'best guess' at the parameter range, the standard deviation in estimated mesozooplankton biomass was never less than 46% of the mean mesozooplankton biomass

estimate but was highest during the spring peak biomass in May and around a secondary biomass peak October to November. The onset of an increase in mesozooplankton biomass in the spring was delayed in Ex. IV
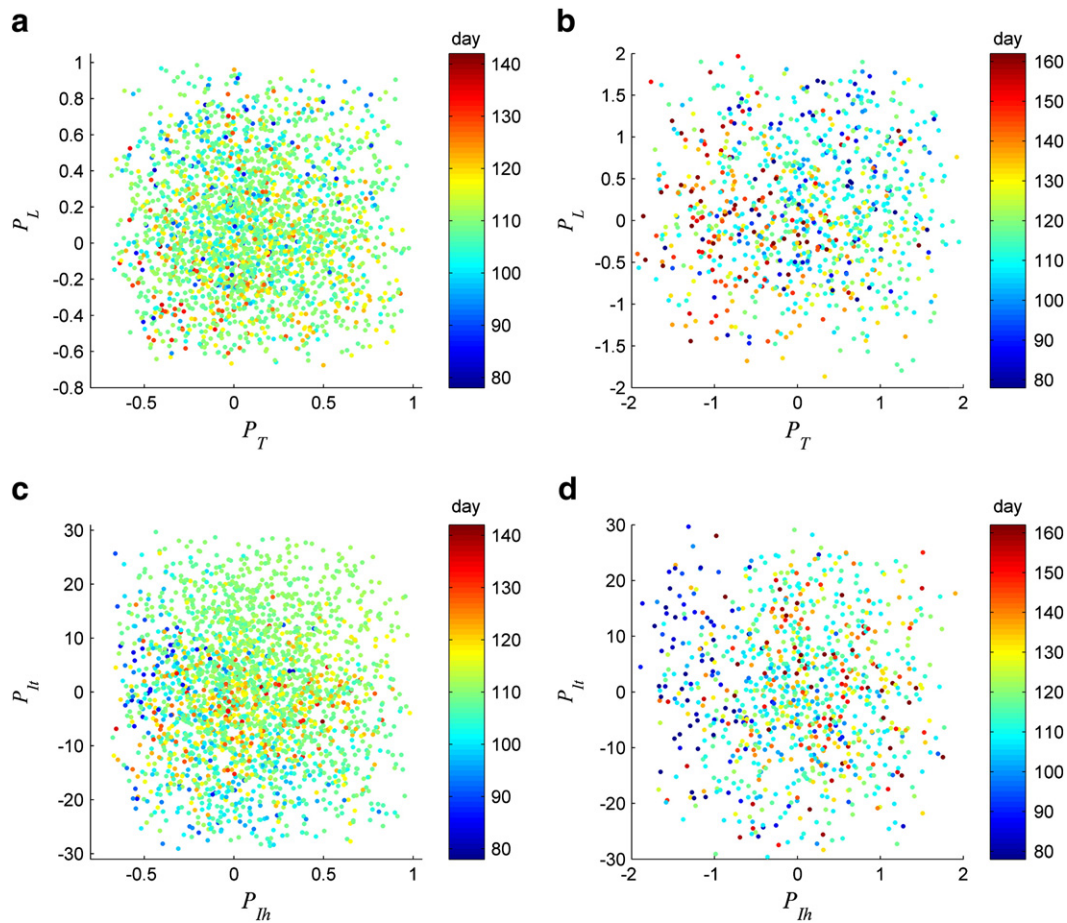
Fig. 4. Scatter plots showing the relationship of *BloomDay* to the temperature (P_T) and light (P_L) parameters for a) Ex. I and b) Ex. IV and the relationship of *BloomDay* (year days) to the ice thickness (P_{Ih}) and ice timing (P_{It}) parameters for c) Ex. I and d) Ex. IV.

a

b
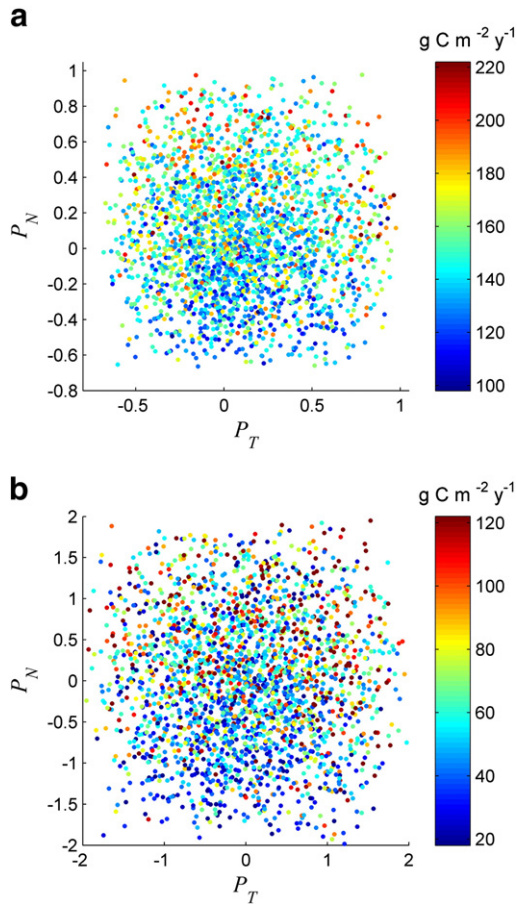
Fig. 6. Scatter plots showing the relationship of net primary production (*NPP*, g C m^{-2} y^{-1}) to the temperature (*P_T*) and initial nitrate (*P_N*) parameters for a) Ex. I and b) Ex. IV. See method text for description of experiments.

a

b

Fig. 7. Relationship between mesozooplankton production (mg C m^{-2} y^{-1}) and *BloomDay* (black data points) and *NPP* (gray data points) for a) Ex. I and b) Ex. IV. See method text for description of experiments.

relative to Ex. I, but the peak biomass of the two experiments coincided in mid-May. Both time series show a decline in biomass following the spring peak that continues through the summer until a second smaller peak at the end of September. With the exception of mid-February to mid-March, when simulated biomass in Ex. IV was significantly less than that simulated in Ex. I, the two time series overlap.

4. Discussion

Sensitivity analysis is a valuable tool for understanding the dynamics of complex ecosystem models. Here we used a Monte Carlo style sensitivity analysis to explore simultaneously the sensitivity of the *BEST–NPZD* lower trophic level ecosystem model outputs to biological model parameters, environmental forcing, and initial conditions. An exploration of the sensitivity of ecosystem model predictions to only the biological model parameters can be very insightful. However, the addition of parameters representing environmental variability, as done here, results in a more complete analysis, providing a measure of the relative importance of biological parameter uncertainty and environmental variability in ecosystem dynamics. This approach has the potential to allow extrapolation of model output to alternate environments and provide insights into likely ecosystem responses that would result from climatic shifts.

Caution should be taken when assessing model parameter sensitivity and impact on the ecosystem response. A typical approach to exploring sensitivity of an ecosystem model has been to vary all model parameters by a fixed percentage from the baseline value (Frost, 1993; Yoshie et al., 2006). Here we have shown that such an approach may not cover the full range of response of the model and may not reveal the true
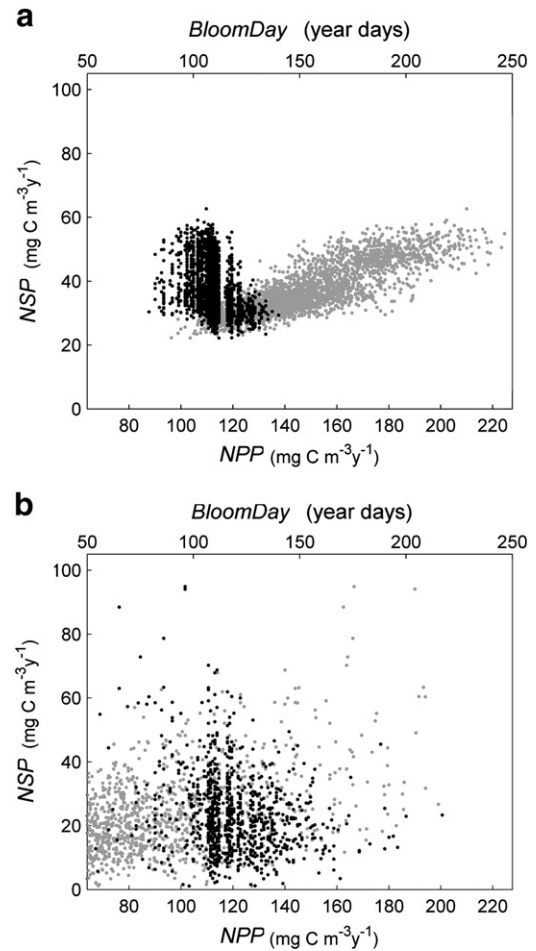
robustness of the model to parameter variation. This becomes apparent only when each parameter is allowed to vary within a more realistic, parameter specific, range. For example, in the *BEST–NPZD* model, parameters determining the fraction of light that is photosynthetically available (*PAR_frac*), the seawater light extinction coefficient (*k_w*), and the Carbon:Chlorophyll-a ratio for phytoplankton (*ccr_PS*, *ccr_PL*) all ranked in the top ten for more than half of the output variables when all parameters were varied by a constant fraction (±60%). Correspondingly, a sensitivity analysis of an ecosystem model with only a single phytoplankton and zooplankton (Frost, 1993) found that a 10% change in attenuation coefficient of irradiance had a near commensurate inverse effect on the rate of primary production, and the Carbon:Chlorophyll-a ratio had a near commensurate effect on depth integrated phytoplankton standing stock. However, we have shown that once each parameter was varied within a more realistic range none of these parameters are highly ranked for any output variable and that parameters previously un-ranked, such as half saturation nutrient uptake coefficients for small phytoplankton (*k_1PS*, *k_2PS*), are revealed as important to model output sensitivity.

The only sensitivity study that we found to vary baseline parameters by non-constant values was an exploration of the sensitivity of a zero dimensional, seven component *NPZD* model applied to Bermuda Station "S" (Fasham et al., 1990), which corresponds to an oligotrophic environment. Using what appears to be a best guess at the parameters' maximum and minimum values, Fasham et al. (1990) found that the most sensitive parameters *NPP* were the slope of the PI curve, the phytoplankton mortality rate, the seawater attenuation coefficient, the
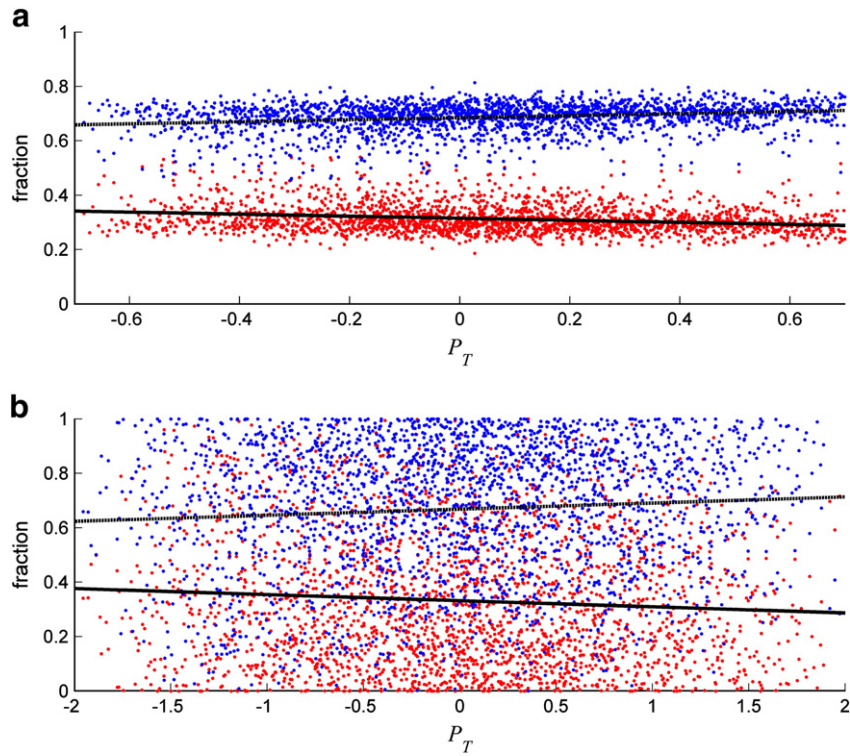
Fig. 8. Fraction of total secondary production (*NSP*, mg C m^{-2} y^{-1}) undertaken by small zooplankton (microzooplankton + small copepods; blue points) vs. large zooplankton (large copepods and euphausiids; red points) for a) Ex. I and b) Ex. IV. See method text for description of experiments.

half saturation uptake for phytoplankton and the sub mixed layer nitrate concentration. As discussed above, with our 'best guess' we did not find the seawater attenuation coefficient to be that important to model output but we did find the slope of the PI curve for small phytoplankton (α_{PS}) to rank in the top 5 for *NPP* along with *Di$_{PS}$*, a parameter used to calculate the small phytoplankton uptake rate in the *BEST–NPZD* model.
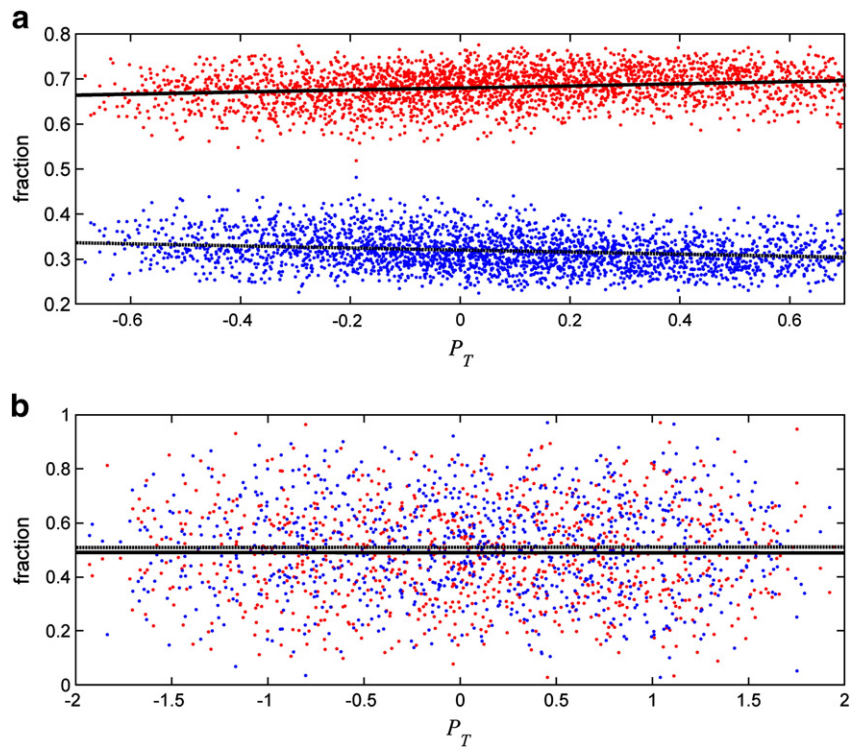
Fig. 9. Fraction of total secondary production (*NSP*, mg C m^{-2} y^{-1}) undertaken by mesozooplankton (small and large copepods and euphausiids; red points) vs. benthic infauna (blue points) for a) Ex. I and b) Ex. IV. See method text for description of experiments.
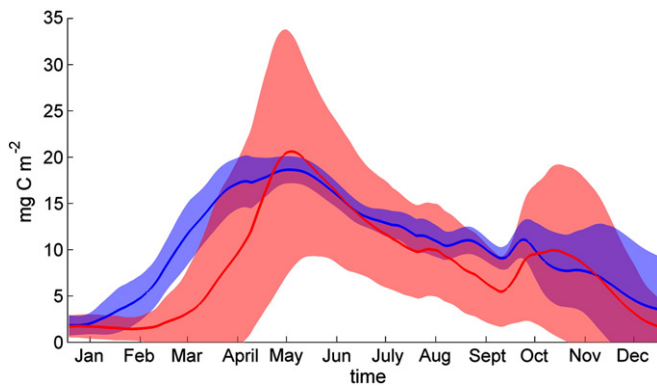
Fig. 10. Mean time series of water column integrated mesozooplankton (Small and large copepods and euphausiids) biomass (mg C m^{-2}) for Ex. I (blue) and Ex. IV (red). Shaded regions indicate ±1 standard deviation from the respective means.

We did not find phytoplankton mortality to rank highly. However, in the *BEST–NPZD* model phytoplankton respiration is explicitly defined and this parameter was a top five ranked parameter for *NPP*. There is no such explicit representation of respiration rate in the Fasham et al. (1990) model so the relative importance of this process could not be determined. The *BEST–NPZD* model is depth explicit so nitrate below mixed layer evolves rather than being explicitly defined. However, in addition to being the number one parameter for nitrate concentration below mixed layer ($[NO_3]_B$), the parameter used to calculate the initial nitrate profile P_N was a top five ranked parameter for *NPP*.

The biological model parameters that were highly ranked depended on the model output to be analyzed. Highly ranked parameters for an output variable were often directly related to this variable, i.e. the biomass of each of the zooplankton groups was influenced by that zooplankton group's own grazing rate, assimilation efficiency and mortality. But, in agreement with Yoshie et al. (2006), we found that the parameter sensitivity structure was often complex in that some parameters had a broad influence, ranking highly for other output variables. For example, the phytoplankton growth parameters (Di_{PS} and Di_{PL}) and microzooplankton grazing rate (e_{ZM}) were ranked within the top five for many of the output variables considered. The physical environment parameter associated with water temperature, salinity, light availability, and ice cover generally did not rank highly for the majority of the considered output variables. This is not to say that these physical characteristics may not be important for ecosystem dynamics, rather that relative to the uncertainty in the biological parameter values the variability in the physical environment plays a more minor role in output uncertainty. The ice thickness (P_{Ih}) was a highly rank physical parameter that could explain >20% of the observed variability in ice algae biomass and potentially 10–20% of the variability in both phytoplankton size classes at the study site. The M2 mooring is located on the middle Bering Sea shelf towards the southern extent of the seasonal ice edge and thus experiences high interannual variability in ice cover. Our results indicate that this variability may play an important role in the phytoplankton dynamics in this region. Strom and Fredrickson (2008) found that warm temperatures, weak winds, and strong stratification are likely to lead to strong nutrient limitation of phytoplankton growth during summer months. However, our analysis indicates that the M2 site will likely see little change in total primary production due solely to rising water temperatures. Sensitivity of the *BEST–NPZD* model to wind forcing was not explored but the lack of temperature control on total productivity suggests that it is the timing and strength of wind events that are more important than temperature in determining water column stratification, nutrient replenishment of the upper mixed layer, and thus overall production of the Bering Sea shelf.

Although total simulated secondary productivity at the M2 study site was not impacted strongly by changes in temperature, there was a shift in the relative contributions of the producers. Our results suggest a shift towards a food web with an increased proportion of the secondary productivity being undertaken by the small zooplankton as water temperature rises. This result is corroborated by Coyle et al. (2008) who found that warmer, more stratified conditions, on the Bering Shelf resulted in significantly enhanced densities of the small copepods and reduced biomass of large copepods and euphausiids relative to colder, less stratified, conditions. As the large bodied zooplankton form an important part of the diet of many Bering Sea fish stocks, i.e., pollock (Moss et al., 2009), such a forecast could have serious implications for the commercial fishing industry in this region.

In the northern Bering Sea ecosystems changes in biological communities contemporaneous with shifts in regional atmospheric and hydrographic forcing have already been observed (Grebmeier et al., 2006). The benthic community and bottom feeders are being replaced by an ecosystem dominated by pelagic fish (Grebmeier et al., 2006). It is not yet known whether the observed decline in prey for benthic feeders, such as whales and walrus, is due to declining productivity and reduced food supply or to top-down control from the benthic feeders themselves (Grebmeier et al., 2006). Our analysis indicates that benthic infaunal production would likely be higher with cooler temperature, and that warming water will cause a shift in the Bering Sea towards a more pelagic-dominated food web. Nonetheless, this temperature response may be outweighed by the inherent variability in the benthic infauna biological process rates. Due to sparse data for the benthic infaunal component, most of the benthic biology parameters were varied within ±60% of their baseline values even within the 'best guess' scenarios. Additional constraints on the benthic infaunal biological process rates would be required to further clarify the relative importance of temperature to the benthic/pelagic shift.

Eastern Bering Sea shelf waters are known to be enriched each winter with deep ocean nutrient-rich water (Whitledge and Luchin, 1999) but winter measurements in the Bering Sea are sparse, making it difficult to develop initial conditions or validate model behavior for this time period. Our results show that initial (winter) nitrate can play an important role in determining the amount of annual net primary production on the Bering Sea shelf. This model sensitivity suggests that changes in the resupply of nutrients to the Bering Sea shelf in winter could have significant consequences for the annual net primary production of the region. Phytoplankton and zooplankton initial conditions were included in our analysis to provide an indication of the sensitivity of model output to the plankton concentrations that remain after winter. Our results indicate that, while these concentrations are not important for the total annual productivity of the ecosystem, they may play a significant role in determining the overall timing of the spring bloom and the biomass of both ice algae and benthos at the study site. Thus, any effort to predict the interannual variability in ecosystem dynamics in high latitude environments needs to carefully consider the biological processes and rates that impact the biomass of overwintering plankton populations.

Our study explored the influence on the lower trophic level Bering Sea ecosystem only within the range of historic temperature variability and present ecosystem structure. We cannot be certain how ecosystem dynamics will respond if, as predicted by some global climate models (IPCC, 2007), water temperatures continue to rise beyond historic levels. It is possible that we will see an introduction of new, better adapted, species with alternate parameter ranges and temperature preferences. Such complexities are not presently captured within the model.

A number of the parameter combinations randomly selected in this study were likely not valid for the Bering Sea ecosystem, as indicated by simulated mean net primary productivity significantly less than the observed net primary production (Rho and Whitledge, 2007) when using the 'best guess' for the parameter ranges (Fig. 5). Strong correlations between input parameters may influence output correlations

(Hamby, 1994); however, correlations between the parameters in lower trophic level marine ecosystem models are not generally known. Therefore, we assumed that all parameters were independent with no correlation among themselves. The addition of correlation information would be of great benefit to sensitivity experiments of this nature by reducing the number of 'false' parameter sets generated and strengthening any conclusions drawn from correlations between parameters and output variables. Determination of parameter correlations would require simultaneous observations for each parameter that are rare or nonexistent. To impose such relationships when selecting input parameter sets would essentially be guess-work and would pre-select for certain ecosystems while eliminating others that may be perfectly valid. Phytoplankton growth and microzooplankton grazing, two of the most sensitive parameters in the *BEST–NPZD* model, have actually been found to be un-correlated, at least at times, on the Bering Sea shelf (Olson and Strom, 2002). Observational data can help constrain ecosystem models by determining which parameters are correlated and which parameter sets are most probable (e.g. Dorner et al., 2009; Matear, 1995, Spitz et al., 1998; 2001). However, parameter optimization was beyond the scope of this study.

Sensitivity analysis, such as the one presented here, helps address uncertainty in ecosystem model outputs due to numerical uncertainty in the parameter values. However, it does not address the additional uncertainty that is inherent in model outputs due to uncertainty about the choice of structural form to represent key biological processes (Walters and Martell, 2004; Wang et al., 2011) nor the choice of the model pathways (Friedrichs et al., 2007; Spitz et al. 2001). Structural uncertainty is much harder to quantify although attempts are being made (Wang et al., 2011). Despite differences in model structure, there is underlying agreement of the most sensitive parameters in the *BEST–NPZD* model and the Nemuro model (Yoshie et al., 2006), a marine ecosystem model of similar complexity. In both instances the parameters determining maximum phytoplankton growth and zooplankton grazing rates were sensitive parameters for many of the output variables examined.

The influence of structural form on ecosystem model dynamics has been explored in some detail for both the zooplankton grazing term (Gibson et al., 2005; Ryabchenko et al., 1997) and the higher level predation (model closure) term (Edwards and Brindley, 1999; Edwards and Yool, 2000). The grazing and predation terms implemented in the *BEST–NPZD* model were selected based on their tendency to promote structurally stable equilibrium solutions comprising all model components with minimal unforced periodic oscillations (Gibson et al., 2005). The *BEST–NPZD* has been designed for coupling with a higher trophic level fish model (*FEAST*) under development through the *BSIERP* research program (http://bsierp.nprb.org). In the one-dimensional uncoupled version of the model presented here, top-down control by higher trophic levels was not explicitly represented. Instead, higher trophic level predation pressure was represented by quadratic model closure terms whose magnitude was influenced by the mortality parameters (m_{ZS}, m_{ZL}, and m_E) and temperature. This structural form essentially represents a predator that exhibits an ambush feeding strategy— a predator attracted to large concentration of zooplankton and less inclined to feed at low concentrations. The mortality parameters ranked within the top five for small and large zooplankton and euphausiid biomass, indicating the potential importance of top-down control in the Bering Sea ecosystem.

Agreement among ecosystem projections from alternative coupled physical–biological models could help gage uncertainty and lend some degree of confidence to ecosystem projections. Although it is becoming increasingly common to consider ensembles of climate forcing scenarios when predicting the likely impact of climate change on physical ocean dynamics (i.e., Wang et al., 2010), this expression of uncertainty is seldom extended to predictions of likely future marine ecosystem dynamics. Fisheries managers have to make difficult decisions related to fisheries openings and total allowable catch in order to balance the sustainability of a fishery with people's livelihoods. To be useful for management applications, confidence estimates or error bars should be a part of any ecosystem projection so that fisheries managers are aware of the associated uncertainty. Although only performed for a one-dimensional version of the *BEST–NPZD* model, our analysis has shown one way in which this can be achieved and the degree of uncertainty in model output that can be expected depending on the uncertainty associated with the model input parameters. To have a true indication of the spatial robustness of the model, this type of sensitivity analysis would have to be performed for the fully three-dimensional physical–biological model. Computational expense at this time precludes running the thousands of three-dimensional model iterations needed for this type of experiment but, if computer development continues at its present rate, this will soon be feasible.

References

Arhonditsis, G.B., Brett, M.T., 2005. Eutrophication model for Lake Washington (USA): part I. model description and sensitivity analysis. Ecol. Model. 187 (2–3), 140–178.

Brodeur, R.R., Sugisaki, H., Hunt Jr., G.L., 2002. Increases in jellyfish biomass in the Bering Sea: implications for the ecosystem. Mar. Ecol. Prog. Ser. 233, 89–103.

Campbell, R.G., Ashjian, C.J., Sherr, B.F., Sherr, E., 2010. Mesozooplankton — Microbial Food Web Interactions in the Bering Sea during Spring Sea-Ice Conditions. Ocean Sciences Meeting, Portland, Oregon, U.S., Oregon Convention Center.

Coyle, K.O., Pinchuk, A.I., 2002. The abundance and distribution of euphausiids and zero-age pollock on the inner shelf of the southeast Bering Sea near the Inner Front in 1997–1999. Deep Sea Res. II 49, 6009–6030.

Coyle, K.O., Konar, B., Blanchard, A., Highsmith, R.C., Carroll, J., Carroll, M., Denisenko, S.G., Sirenko, B.I., 2007. Potential effects of temperature on the benthic infaunal community on the southeastern Bering Sea shelf: possible impacts of climate change. Deep Sea Res. II 54 (23–26), 2885–2905.

Coyle, K.O., Pinchuk, A.I., Eisner, L.B., Napp, J.M., 2008. Zooplankton species composition, abundance and biomass on the eastern Bering Sea shelf during summer: the potential role of water-column stability and nutrients in structuring the zooplankton community. Deep Sea Res. II 55, 1775–1791.

Denman, K.L., Peña, M.A., Haigh, S.P., 1998. Simulations of marine ecosystem response to climate variation with a one dimensional coupled ecosystem/mixed layer model. Biotic Impacts of Extratropical Climate Variability in the Pacific. Proceedings 'Aha Huliko'a Hawaiian Winter Workshop, University of Hawaii at Manoa. pp. 141–147.

Dorner, B., Peterman, R.M., Zhenming, S., 2009. Evaluation of performance of alternative management models of Pacific salmon (*Oncorhynchus* pp.) in the presence of climatic change and outcome uncertainty using Monte Carlo simulations. Can. J. Fish. Aquat. Sci. 66 (12), 2199–2221.

Ebenhöh, W., Kohlmeier, C., Radford, P.I., 1995. The benthic biological submodel in the European Regional Seas Ecosystem Model. Netherlands. J. Sea Res. 33 (3–4), 423–452.

Edwards, A.M., Brindley, J., 1999. Zooplankton mortality and the dynamical behaviour of plankton population models. B. Math. Biol. 61, 303–339.

Edwards, A.M., Yool, A., 2000. The role of higher predation in plankton population models. J. Plankton Res. 22, 1085–1112.

Fasham, M.J.R., Ducklow, H.W., McKelvie, S.M., 1990. A nitrogen-based model of plankton dynamics in the oceanic mixed layer. J. Mar. Res. 48, 591–639.

Friedrichs, M.A.M., Dusenberry, J.A., Anderson, L.A., Armstrong, R., Chai, F., Christian, J.R., Doney, S.C., Dunne, J., Fujii, M., Hood, R., McGillicuddy, D., Moore, J.K., Schartau, M., Spitz, Y.H., Wiggert, J.D., 2007. Assessment of skill and portability in regional marine biogeochemical models: the role of multiple planktonic groups. J. Geophys. Res. 112, C08001. doi:10.1029/2006JC003852.

Frost, B.W., 1993. A modelling study of processes regulating plankton standing stock and production in the open subarctic Pacific Ocean. Prog. Oceanogr. 32 (1–4), 17–56.

Gibson, G.A., Musgrave, D.L., Hinckley, S., 2005. Non-linear dynamics of a pelagic ecosystem model with multiple predator and prey types. J. Plankton Res. 27 (5), 427–447.

Grebmeier, J.M., Overland, J.E., Moore, S.E., Farley, E.V., Carmack, E.C., Cooper, L.W., Frey, K.E., Helle, J.H., McLaughlin, F.A., McNutt, S.L., 2006. A major ecosystem shift in the northern Bering Sea. Science 311 (5766), 1461–1464.

Haidvogel, D.B., Arango, H., Budgell, W.P., Cornuelle, B.D., Curchitser, E., Di Lorenzo, E., Fennel, K., Geyer, W.R., Hermann, A.J., Lanerolle, L., Levin, J., McWilliams, J.C., Miller, A.J., Moore, A.M., Powell, T.M., Shchepetkin, A.F., Sherwood, C.R., Signell, R.P., Warner, J.C., Wilkin, J., 2008. Regional ocean forecasting in terrain-following coordinates: model formulation and skill assessment. J. Comput. Phys. 227, 3595–3624.

Hamby, D.M., 1994. A review of techniques for parameter sensitivity analysis of environmental models. Environ. Monit. Assess. 32, 135–154.

Hansson, L.J., Kiørboe, T., 2006. Effects of large gut volume in gelatinous zooplankton: ingestion rate, bolus production and food patch utilization by the jellyfish *Sarsia tubulosa*. J. Plankton Res. 28 (10), 937–942.

Hinckley, S., Coyle, K.O., Gibson, G., Hermann, A.J., Dobbins, E.L., 2009. A biophysical NPZ model with iron for the Gulf of Alaska: reproducing the differences between an oceanic HNLC ecosystem and a classical northern temperate shelf ecosystem. Deep Sea Res. II 56 (24), 2520–2536.

IPCC, 2007. Climate Change 2007: The Physical Science Basis. In: Solomon, S., Qin, D., Manning, M., Chen, Z., Marquis, M., Tignor, K.B.M., Miller, H.L. (Eds.), Contribution of Working Group I to the Fourth Assessment Report of the Intergovernmental Panel on Climate Change. Cambridge University Press, Cambridge, United Kingdom and New York, NY, USA, p. 996.

Jin, M., Deal, C., Wang, J., Shin, K.H., Tanaka, N., Whitledge, T., Lee, S.H., Gradinger, R., 2006. Controls of the land fast ice-ocean ecosystem offshore Barrow. Alaska. Ann. Glaciol. 44, 63–72.

Large, W.G., Yeager, S.G., 2009. The global climatology of an interannually varying air–sea flux data set. Clim. Dynam. 33, 341–364.

Lessard, E., Shaw, C.T., Bernhardt, M.J., Engel, V.L., Foy, M.S., 2010. Euphausiid Feeding and Growth in the Eastern Bering Sea, Feb 24 2010. Ocean Sciences Meeting, Portland, Oregon, U.S., Oregon Convention Center.

Lomas, M.W., Glibert, P.M., 1999. Temperature regulation of nitrate uptake: a novel hypothesis about nitrate uptake and reduction in cool-water diatoms. Limnol. Oceanogr. 44, 556–572.

Matear, R.J., 1995. Parameter optimization and analysis of ecosystem models using simulated annealing: a case study at Station P. J. Mar. Res. 53, 571–607.

Megrey, B.A., Hinckley, S., 2001. The effect of turbulence on feeding of larval fishes: a sensitivity analysis using an individual-based model. ICES J. Mar. Sci. 58, 1015–1029.

Moore, A.M., Arango, H.G., DiLorenzo, E., Cornuelle, B.D., Miller, A.J., Neilsen, D.J., 2004. A comprehensive ocean prediction and analysis system based on the tangent linear and adjoint of a regional ocean model. Ocean Model. 7, 227–258.

Moss, J.H., Farley Jr., E.V., Feldmann, A.M., Ianelli, J.N., 2009. Spatial distribution, energetic status, and food habits of eastern Bering Sea age-0 walleye pollock. T. Am. Fish. Soc. 138, 497–505.

Olson, M.B., Strom, S.L., 2002. Phytoplankton growth, microzooplankton herbivory and community structure in the southeast Bering Sea: insight into the formation and temporal persistence of an *Emiliania huxleyi* bloom. Deep Sea Res. II 49, 5969–5990.

Pauly, D., Graham, W., Libralato, S., Morissette, L., Palomares, M.L.D., 2009. Jellyfish in ecosystems, online databases, and ecosystem models. Hydrobiologia 616, 67–85.

Rho, T., Whitledge, T.E., 2007. Characteristics of seasonal and spatial variations of primary production over the southeastern Bering Sea shelf. Cont. Shelf Res. 27, 2556–2569.

Rose, K.A., Smith, E.P., Gardner, R.H., Brenkert, A.L., Bartell, S.M., 1991. Parameter sensitivities, Monte Carlo filtering, and model forecasting under uncertainty. J. Forecasting 10, 117–133.

Ryabchenko, V.A., Fasham, M.J.R., Kagan, B.A., Popova, E.E., 1997. What causes short-term oscillations in ecosystem models of the ocean mixed layer? J. Mar. Res. 13 (1–4), 33–50.

Shchepetkin, A.F., McWilliams, J.C., 2005. The Regional Ocean Modeling System: a split-explicit, free-surface, topography-following coordinate ocean model. Ocean Model. 9 (4), 347–404.

Sobol, I.M., 1994. A Primer for the Monte Carlo Method. FL: CRC Press, Boca Raton, p. 128.

Soetaert, K., Middelburg, J.J., Herman, P.M.J., Buis, K., 2000. On the coupling of benthic and pelagic biogeochemical models. Earth Sci. Rev. 51 (1–4), 173–201.

Spitz, Y.H., Moisan, J.R., Abbott, M.R., Richman, J.G., 1998. Data assimilation and a pelagic ecosystem model: parameterization using time series observations. J. Mar. Syst. 16 (1–2), 51–68.

Spitz, Y.H., Moisan, J.R., Abbott, M.R., 2001. Configuring an ecosystem model using data from the Bermuda-Atlantic Time Series (BATS). Deep Sea Res. II 48, 1733–1768.

Stabeno, P.J., Bond, N.A., Kachel, N.B., Salo, S.A., Schumacher, J.D., 2001. On the temporal variability of the physical environment over the south-eastern Bering Sea. Fish. Oceanogr. 10 (1), 81–98.

Strom, S.L., Fredrickson, K.A., 2008. Intense stratification leads to phytoplankton nutrient limitation and reduced microzooplankton grazing in the southeastern Bering Sea. Deep Sea Res. 55, 1761–1774.

Sukhanova, I.N., Semina, H.J., Venttsel, M.V., 1999. Spatial distribution and temporal variability of phytoplankton in the Bering Sea. In: Loughlin, T.R., Ohtani, K. (Eds.), Dynamics of the Bering Sea. University of Alaska Sea Grant, AK-SG-99-03, Fairbanks, pp. 193–215.

Trites, A.W., Livingston, P., Vasconcellos, M.C., Mackinson, S., Springer, A.M., Pauly, D., 1999. Ecosystem Change and the Decline of Marine Mammals in the Eastern Bering Sea: Testing the Ecosystem Shift and Commercial Whaling Hypotheses. Fisheries Centre Research Reports. 7, 106 pp.

Uye, S., Shimauchi, H., 2005. Population biomass, feeding, respiration and growth rates, and carbon budget of the scyphomedusa *Aurelia aurita* in the Inland Sea of Japan. J. Plankton Res. 27 (3), 237–248.

Verbeeck, H., Samson, R., Verdonck, F., Lemeur, R., 2006. Parameter sensitivity and uncertainty of the forest carbon flux model FORUG: a Monte Carlo analysis. Tree Physiol. 26 (6), 807–817.

Vidal, J., Smith, S.L., 1986. Biomass, growth, and development of populations of herbivorous zooplankton in the southeastern Bering Sea during spring. Deep Sea Res. I 33 (4A), 523–556.

Walsh, J.J., McRoy, C.P., 1986. Ecosystem analysis in the southeastern Bering Sea. Cont. Shelf Res. 5, 259–288.

Walsh, J.J., Rowe, G.T., Iverson, R.L., McRoy, C.P., 1981. Biological export of shelf carbon is a sink of the global CO_2 cycle. Nature 291, 196–201.

Walters, C.J., Martell, S., 2004. Fisheries Ecology and Management. Princeton University Press, Princeton, New Jersey.

Wang, M., Overland, J.E., Bond, N.A., 2010. Climate projections for selected large marine ecosystems. J. Mar. Syst. 2 (3–4), 258–266.

Wang, W., Dungan, J., Hashimoto, H., Michaelis, A.R., Milesi, C., Ichii, K., Nemani, R.R., 2011. Diagnosing and assessing uncertainties of terrestrial ecosystem models in a multi-model ensemble experiment: 1. primary production. Global Change Biol. 17, 1367–1378.

Whitledge, T.E., Luchin, V.A., 1999. Summary of chemical distributions and dynamics in the Bering Sea. In: Loughlin, T.R., Ohtani, K. (Eds.), Dynamics of the Bering Sea. Univ. Of Alaska Sea Grant, Fairbanks, Alaska, pp. 217–249.

Yoshie, N., Yamanaka, Y., Rose, K.A., Eslinger, D.L., Ware, D.M., Kishi, M.J., 2006. Parameter sensitivity study of the NEMURO lower trophic level marine ecosystem model. Ecol. Model. 202, 26–37.